Copper smelting technology at 2nd millennium BC Taldysai (Kazakhstan) and its place in the wider Eurasian metalmaking framework

Ilaria Calgaro[a,*], Miljana Radivojević[a], Umberto Veronesi[b], Antonina S. Yermolayeva[c]

[a] Institute of Archaeology, University College London, 31-34 Gordon Square, London WC1H 0PY, UK
[b] VICARTE Research Unit, Faculty of Science and Technology, Universidade Nova de Lisboa, 2829-516 Caparica, Portugal
[c] A.Kh. Margulan Institute of Archaeology, Almaty 050010, Kazakhstan
* ilaria.calgaro.19@ucl.ac.uk

Abstract

The 2nd millennium BC in the Eurasian Steppe has widely been recognised as the period of exponential surge in circulation of metals, as well as metal exploitation activities across this area. Nevertheless, there is a general paucity of data on metal production in the steppes, which comes in as crucial in the interpretation of the role metalmaking played in the Bronze Age Eurasian Steppe communities.

Here we report analyses of a pilot sample of nine smelting slags from the 2nd millennium BC metalmaking workshop of Taldysai in Central Kazakhstan. Our preliminary results identified at least two metal production lines: copper and arsenical copper. Copper metal was obtained by co-smelting copper oxides and sulfides most likely originating from local cuprous sandstone in a single step. Arsenical copper production is exhibited through co-smelting of copper and arsenic-rich ores in two steps, one to remove sulfur, the second to release the iron present in the charge.

Compared against a reference database of nine 2nd millennium BC Bronze Age metal production sites across Eurasia, our results suggest that metalsmiths had mastered multiple ways to extract copper-based alloys: by combining raw materials in different recipes, applying diverse pyrotechnological solutions and exploiting a variety of locally and regionally available ores. This perspective allows for postulating local inventiveness at play for copper and copper alloy production in the Bronze Age steppes, and beyond.

Keywords (3-7)

Middle-Late Bronze Age - copper smelting - arsenical copper - Taldysai - Eurasian Steppe - chemical analysis

1. Introduction

The Bronze Age in the Eurasian Steppe was one of the most dynamic periods in the history of the continent. It was the arena for the spread of populations, diseases, genes, horse riding and chariots, as well as the trade of commodities such as semiprecious stones, textiles and, most prominently, metals (e.g. Chernykh, 1992; Khazanov, 1994; Di Cosmo, 1996: 87; Anthony, 2007; Frachetti, 2012; Chernykh 2013; Allentoft et al. 2015; Haak et al., 2015; Frachetti et al., 2017; Narasimhan et al., 2019; Shishlina et al., 2020; Librado et al., 2021).

It was this enhanced dynamic in trade and exchange that prompted Vandkilde (2016; 2017) to see the Bronze Age as an early form of globalisation, or *Bronzization*, comparable in scale and reach to Neolithisation, Mediterranisation, Romanisation, and other terms often employed to refer to the interconnectivity phenomena in ancient times. The Bronzization label would make specific reference to the desire and demand for copper alloys for warfare, ritual, economic and daily use, thus indicating the largest pre-modern 'globalising' network characterising Eurasia during the second part of the 2nd millennium BC (1600-1200 BC).

It is usually acknowledged that by this time, which corresponds to the Mid-Late Bronze Age, the mastering of copper metallurgy in terms of metal extraction from ores, process standardisation, large-scale production and consumption of finished metal artefacts, had reached its peak (Chernykh, 1992: 3135).

Semi-nomadic pastoralist communities of the Eurasian Steppe have been considered as the major suppliers of copper metal alloys in the Eurasian continent during the Bronze Age (Chernykh, 2008; Chernykh, 2011; Chernykh, 2013). The 2nd millennium BC has widely been recognised as the period of exponential surge in the circulation of metals, as well as metal exploitation activities across Eurasia (e.g. Chernykh, 2007; Stöllner et al., 2013a; 2013b; Pernicka et al., 2016; Vandkilde, 2016; Radivojević et al., 2019). Nevertheless, there is a general paucity of data related to metal production in the steppes, which comes in as crucial in the interpretation of the role metalmaking played in the Bronze Age Eurasian Steppe communities. In this sense, the characterisation of metalmaking technology is key to inform on the raw and finished materials supply networks underlying the circulation of goods throughout this continent.

Thus far the evolution of the Bronze Age Eurasian Steppe metallurgy has been traditionally approached through extensive typologies of artefacts and characterisation of metal ore deposits, which led to the theorisation of a staged development of metallurgy adoption and expansion from West to East via production cores, labelled as 'metallurgical provinces' (Chernykh, 1992; Chernykh, 2011).

Nevertheless, most of the recent studies as well have concentrated on the characterisation of metal artefacts instead of production debris, barring a few examples including the analyses of metallurgical debris from Bronze Age mining sites and settlements in the Urals, such as the case of Kargaly, the Mugodzhary region in southern Urals and Askaraly, the tin mine in east Kazakhstan (Chernykh, 2002a; 2002b; 2004; Hanks and Doonan, 2009; Stöllner et al., 2013a; 2013b; Tkachev et al. 2014; Anthony et al. 2016; Tkachev, 2019; Ankushev et al. 2021).

The analysis of metal production debris is key to understand smelting recipes, traditions, and mechanisms of their transmission through time, and ultimately a complex interaction between resources, environment and communities. Given that production debris are waste, they are usually found *in situ* and unlikely to travel, hence representing the most reliable source of information about the knowledge of metalmaking.

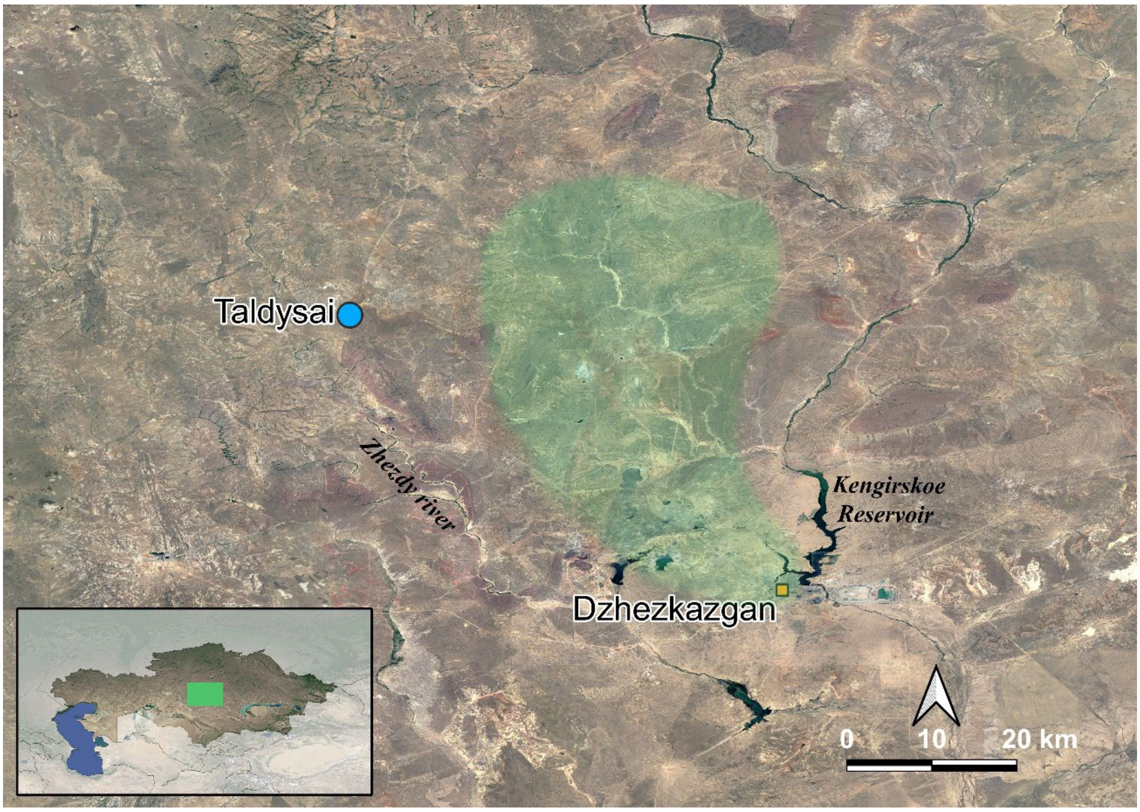

Fig. 1. Geographic location of Taldysai and of the modern city of Dzhezkazgan in central Kazakhstan. The extension of the Dzhezkazgan copper ore field, including modern prospection areas, is shaded in green. (source: Mindat https://www.mindat.org/feature-1516589.html).

This study focuses on the site of Taldysai (**Figure 1**), a metal production site located in the Central Kazakhstan steppes, dated between 1900 to 1200 BC. The settlement includes a series of workshops and has thus far yielded extensive evidence of raw materials such as copper minerals, metallurgical waste products in form of smelting slags, casting debris and finished metal artefacts, largely related to the initial stages of its life, from ca 1900 to1600 BC (Kurmankulov et al., 2012; Yermolayeva et al. 2020).

Since ideas and concepts about the Bronze Age metallurgy are usually discussed in the light of trade of metal artefacts (e.g. Chernykh and Kuzminykh, 1989; Kohl, 2007; Kuzmina, 2008; Vandkilde, 2016; 2017), further aim of this paper is to contribute to the understanding of metalmaking technology in the 2nd millennium BC. We do so by comparing the analysis of Taldysai production to that of nine co-eval production centres across Eurasia and discussing a common baseline for metal production technology at the time.

2. The settlement of Taldysai. Archaeological context, geology and metal production

The Bronze Age in the Eurasian Steppe covers a timeframe which spans ca 3500-1000 BC. It may be roughly sub-divided into Early (EBA,~3500-2500 BC), Middle (MBA,~2500-1900 BC), Late (LBA,~1900-1500 BC) and Final (FBA,~1500-1000 BC) in the steppes, though with regional variations. This paper deals with metal production of Mid/Late Bronze Age related to the Petrovka and Alakul-Fedorovo cultural horizons at Taldysai. The Petrovka horizon starts at c. 1900 BC, while Alakul-Fedorovo materials are noted from c. 1800 BC and last until 1600 BC. Petrovka and Alakul-Fedorovo cultural groups are also recognised in Central Kazakhstan as Nurtai (Petrovka), Atasu (Alakul) and Nura (Fedorovo), which identify equivalent local pottery variants (Yermolayeva et al., 2020; Grigoriev, 2021).

The site of Taldysai is located in the Ulytau district of the Karaganda oblast in Central Kazakhstan, c. 70 km from the copper mining district of Dzhezkazgan (**Figure 1**). The ore field of Dzhezkazgan is extended across c. 100 km^2. It is part of the Chu-Sarysu basin and includes traces of copper mining since at least 1500 BC (Box et al., 2012a; Margulan, 2020). The Dzhezkazgan mineralisation occurred through hydrothermal processes, i.e. via hydrothermal solutions enriched with sulfur and iron rising along cracks of quartz veins, then forming stratiform layers of primary Cu and Cu-Fe sulfides (pyrite FeS_2, chalcopyrite $CuFeS_2$, bornite Cu_5FeS_4 and chalcocite Cu_2S), then horizons of secondary copper sulfides such as bornite, chalcocite and covellite (which reach up to 60-70 m, Grigoriev, 2015: 505) intermixed with sandstone, shale, limestone and dolomite beds, and an oxidised zone of copper oxides and carbonates at the top (Copper Fields of Kazakhstan, 1997: 49; Box et al., 2012b; Ankushev et al., 2020). Near present-day surface the accumulations of secondary oxidised copper ores reach 5-6 m of thickness (or up to 8-12 m as reported by Ankushev et al., 2020) (Satpaev 1935: 211, 219; Grigoriev, 2015: 505). The oxidised horizon includes copper minerals such as malachite ($Cu_2CO_3(OH)_2$), azurite ($C_2H_2Cu_3O_8$), cuprite (Cu_2O), chrysocolla ($CuSiO_3 \cdot 2H_2O$), native copper, but also iron oxides and hydroxides mineralised in grey sandstone and quartz veins of 1-2 cm thickness. The content of copper in the oxidic ore ranges between 5-35% (Grigoriev, 2015), which is also consistent with atomic absorption and Induced Coupled Plasma Mass Spectrometry (ICP-MS) analysis of copper oxides found at Taldysai analysed by Ankushev et al. (2020), who reported a Cu content oscillating between 30-38%. It is worth mentioning that Satpaeva (2007) identified the presence of arsenic, mercury and silver upon core drilling at Dzhezkazgan (up to 450-500 m in depth), although it is unknown whether these horizons were exploited in prehistory. A clear assessment of the horizons mined during the Bronze Age is also complicated by the stratiform nature of the deposit itself (Stöllner, 2018: 102, Figure 12).

Taldysai came to light in 1990 following a water flood of the Bala Zhezdy and Ulken Zhezdy rivers in its proximity, which also cut a channel through the southern half of the settlement, hence this part of the site is affected by a high degree of disturbance and materials mixing. Archaeological investigations started in 1994, conducted by the Central Kazakhstan Archaeological Expedition of the A.Kh. Margulan Institute of Archaeology of Almaty, first directed by Dr Zh. Kurmankulov and then by Dr A.S. Yermolayeva (Kurmankulov et al., 2012; Artyuhova et al., 2013; Yermolayeva et al., 2013; Yermolayeva, 2020). Three metallurgical complexes (sets of workshops) were unearthed at Taldysai thus far, called the eastern, western and northern complexes, which functioned at different stages of the 2nd millennium BC. Excavation 1 includes all complexes and is presented with the largest excavation trench in **Figure 2**. Excavation 2 was opened to investigate the westernmost destroyed half of the settlement, whereas Excavation 3, located on the opposite bank of the river, followed the structure of some smelting furnaces eroded by the floods (**Figure 2** - Yermolayeva et al., 2020a). The overall interpretation of the discovered features is that they all belong to metallurgical installations, whereas separate dwelling features have not yet been discovered. The excavators assume that the metalsmiths either lived in the workshops, or more likely, in yet to be excavated housing structures (Yermolayeva, 2020: 4).

The northern complex in Excavation 1 corresponds to the first phase of life and metal production operations at the site. This area is securely attributed to the Middle Bronze Age Petrovka culture of the first half of the 2nd millennium BC (Yermolayeva, 2016; Yermolayeva, 2017; Yermolayeva et al., 2018; Yermolayeva et al., 2019; Yermolayeva et al., 2020b). On the other hand, western and eastern complexes of the Excavation 1 are affected by severe mixing of materials from Mid/Late Bronze Age and are more damaged by the action of the rivers, as water floods eroded the southern sides of both these sectors. The ceramic materials here are typo-chronologically attributed to the Petrovka (Nurtai), and later to early Alakul (Atasu) and Fedorovo (Nura) cultural horizons and appear mixed up.

Fig. 2. (a) Aerial view of the site of Taldysai, showing (1) western (2) eastern (3) northern complexes in Excavation 1 and (4) Excavation 2, (5) Excavation 3. The unearthed features are solely metal workshop debris (Modified from Yermolayeva, 2020: 14, Photo 3).

Excavations at Taldysai unearthed a series of pits of different sizes serving various purposes, i.e. metallurgical furnaces, water wells, domestic hearths, waste disposal and/or sacrificial depositions of animal remains. The animal remains are ascribed to the latest occupational horizon, Sargary-Alekseevka, which does not include primary metal production described in this paper, and out of the scope of research presented here (**Figure 3**; Yermolayeva, 2016; Yermolayeva et al., 2019). Three types of smelting structures were identified across Petrovka and Alakul-Fedorovo horizons: vaulted pit furnaces, with pit varying in size ('*shahtnovo'* – larger - and '*polushahtnovo tipa*', - smaller, hence vaulted 'semi' pit furnace), and bowl-shaped above-ground furnaces ('*nadzemnovo tipa*'; Yermolayeva, 2016; 2017) (**Figure 3**). All three types of smelting structures are present in the northern complex from the initial stage of the settlement.

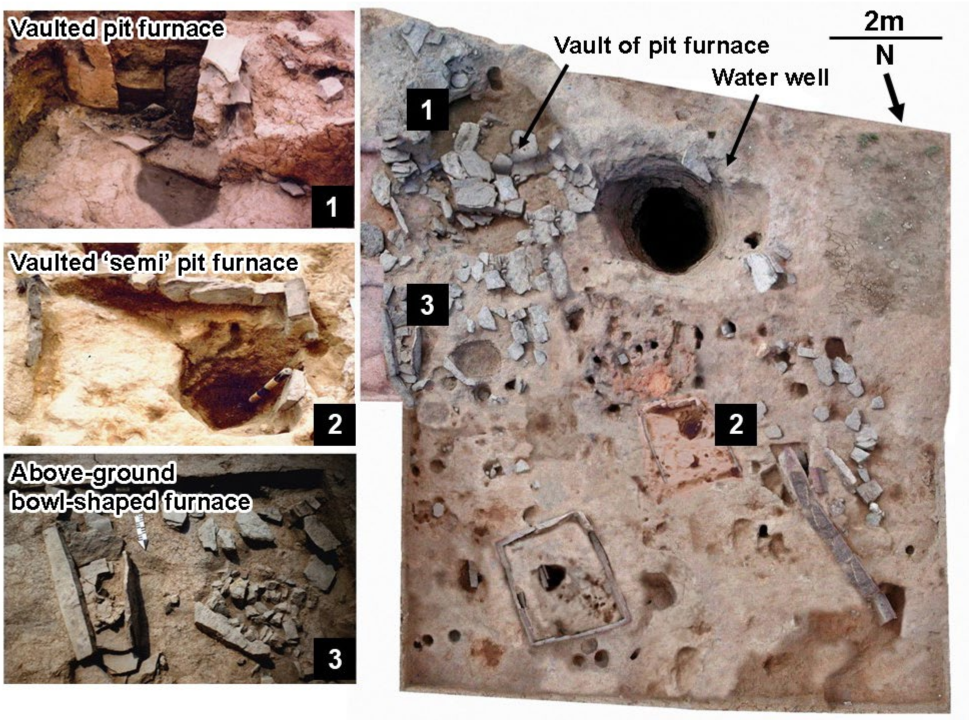

Fig. 3. Examples of the three types of smelting furnaces unearthed at Taldysai in the western complex (1) top (righ) and inside (left) view of pit furnace ('shahtnovo' type). Note in the orthophoto on the right the vault covering of the furnace structure shown on the left (before and after excavation); (2) top view of smaller pit furnace ('polushahtnovo' type) upon excavation; (3) above-ground bowl-shaped furnace enclosed in stone slabs. Modified from Yermolayeva et al. (2020a: 43, Photo 1) and Kurmakulov et al. (2012: 77; 86) and courtesy of A.S. Yermolayeva.

The vaulted pit furnaces at Taldysai consist of ground pits reaching down to 2 m in depth and a system of inner radial ducts alongside the walls (**Figures 3, 4a-b**). They are covered by a vault made of stone slabs and plaster (**Figure 3**) and accompanied with a horizontal channel that varies in length (up to 8 meters) (**Figures 4, 5**). Experimental reconstruction of these furnaces, based on detailed fieldwork reports, was successfully built and ran by I. Rusanov (Artyuhova et al., 2013; Yermolayeva and Rusanov, 2022). **Figure 4c** shows the cross section of this experimental furnace, which also features a chimney at the far end of the 8.5 m horizontal channel (or the exit). These trials offer a valid reconstruction of the functioning of such structures. This furnace was loaded through a top hole left in the vault to access the pit with ores and fuel. To start the extraction process, a fire (red ellipse on the right, **Figure 4c**) was started at the far end of the horizontal channel (the exit) in order to pre-heat the air and hence create a difference in pressure between the channel exit and the pit. After this, the fire was also set to the loaded pit (red ellipse on the left, **Figure 4c**), where the system of inner radial ducts provided a fresh air-supply needed for the combustion of the fuel and reduction of the ores (**Figure 4a-b**).

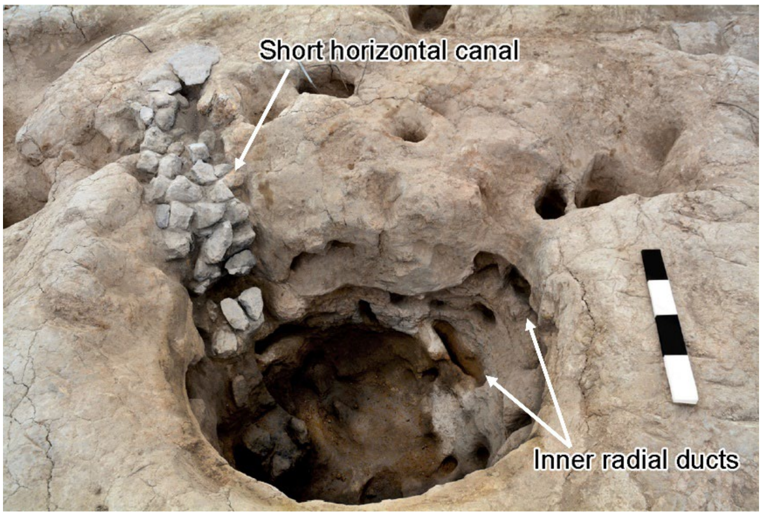

(a)

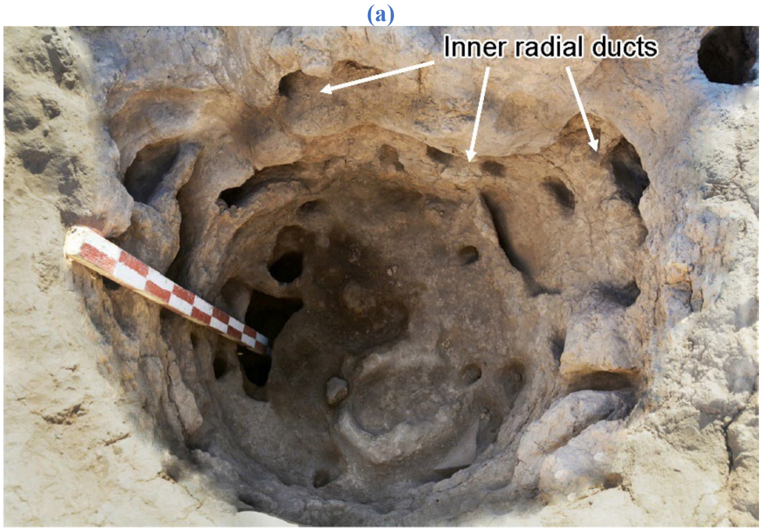

(b)

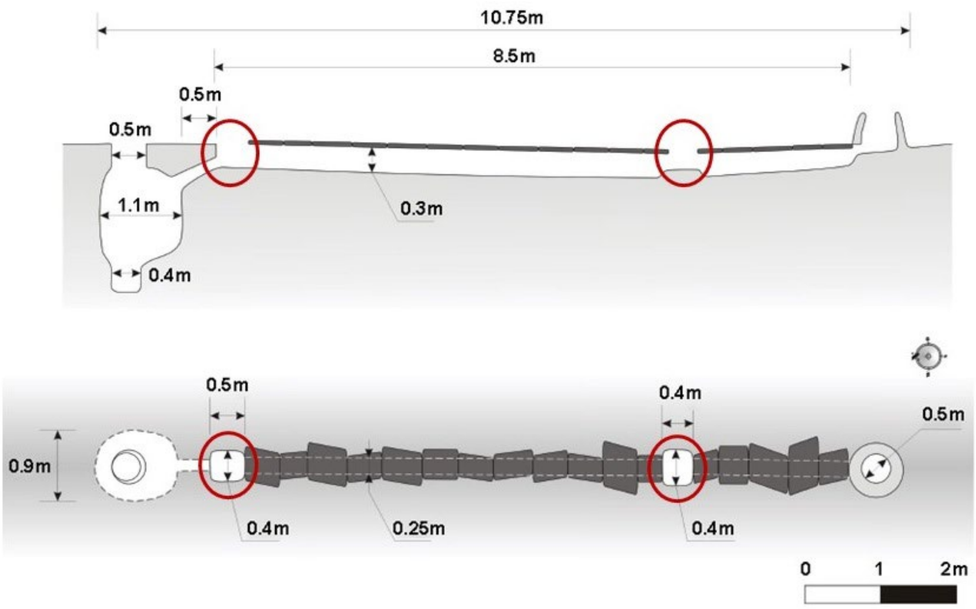

(c)

Fig. 4. (a-b) Example of semi-pit furnace ('polushahtnovo tipa') from the northern complex of Taldysai with a short horizontal canal covered in stones connected to the pit structure through a horizontal hole in the ground. An inner system of radial and vertical ducts providing fresh-air supply is visible in form of cuts in the soil alongside the profile of the pit furnace (modified from Yermolayeva et al., 2020a: 65-66, Figures 23, 24). (c) Section of the experimental pit furnace (left end) with horizontal channel and

chimney (right end) reconstructed by I. Rusanov in 2012 at Taldysai (modified from Yermolayeva and Rusanov, 2022: 88-89, Figure 2)

Due to the negative pressure gradient in the pit furnace and the exit of the channel (chimney), the fumes from the metal extraction were diverted towards the latter. In this way no forced ventilation systems or devices were needed to push the inlet of fresh air (e.g. bellows). Hence, the horizontal channel served two purposes, *(i)* it facilitated the pressure difference across the furnace structure; *(ii)* it provided safety for the metalsmiths by diverting fumes from smelting (**Figures 4c, 5**). Once reduced, the smelted metal (i.e. black copper, below) was recovered from the bottom of the pit-furnace (Yermolayeva et al., 2020).

***Fig. 5.** Three-chambers pit furnace unearthed in the northern complex of Taldysai (top centre of the picture). A horizontal canal covered in stones departs from the furnace and comes towards the bottom centre of the picture (modified from Yermolayeva, 2016: 35, Figure 9).*

These pit furnaces have been recovered with a single or up to three chambers in Taldysai (**Figure 5**). At present, typological comparisons to this type of furnace structures are widespread from Eastern Europe to Central Asia, i.e. from the Donetsk region via Southern Urals (Sintashta and Arkaim) (Grigoriev, 2000; Grigoriev and Rusanov, 1995), the Central Kazakhstan steppes (Atasu, Myrzhik, Akmaya and Akmustafa) (Kadyrbaev, 1983; Kuznetsova and Teplovodskaya, 1994; Beisenov et al., 2017; Yermolayeva, 2017) to the Zarafshan Valley (Tugai) in Uzbekistan (Avanesova, 2015; 2020; Avanesova, pers. comm.). Grigoriev (2015: 97) hypotheses that the appearance of the horizontal channel in Sintashta furnaces might have been a solution to drive off sulfur dioxide gases if sulfides were included in the ore charge, since a chimney would not represent an essential requirement when smelting copper oxidic ores, an aspect that we will discuss further in this paper. Noteworthy, Kuznetsova and Teplovodskaya (1994: 51-44) propose that these furnaces at Atasu would have needed tuyeres and bellows to enhance the air supply; however, no material evidence thus far supports this.

In addition to the pit furnaces detailed above, smaller bowl-type furnaces were found at Taldysai (**Figure 6**), often enclosed within stone slabs (**Figure 3**). These structures were found in the vicinity of the pit furnaces, filled with sooty stones, ashes, calcinated animal bones and ceramic fragments. Moreover, these furnaces present a side hole, likely to be used to insert a nozzle (presumably connected to a leather bag or a bellow). Both furnaces and nozzles have been recovered *in situ* and are generally characterised by a poor state of preservation (**Figure 6**; Yermolayeva, 2016: 132; 2017). Casting of finished metal artefacts was also performed at the site, as exhibited by the numerous items found within the settlement such as knives, arrowheads, staples, beads, ingots, chisels, awls, alongside production tools such as crucibles, pestles, mortars, casting moulds and copper ores (Kurmankulov et al., 2012; Yermolayeva et al., 2019).

Fig. 6. Bowl-shaped above-ground smelting furnaces ('nadzemnovo tipa') from the western complex in Taldysai. The clay structure includes the opening for the nozzle insertion in the upper wall (from Yermolayeva et al., 2020a: 54, Photo 12, 2).

By the 2nd half of the 2nd millennium BC, the use of the vaulted pit furnaces and bowl-type installation ceases; they were discovered as completely filled with rubble (Yermolayeva, 2016: 133-136). The last phase of Taldysai occupation is the Late Bronze Age Sargary nomadic culture of Central/Eastern Kazakhstan, dated between 1600-1400 cal BC (Hermes et al., 2020). In this phase the economy of the settlement shifts strictly to cattle-breeding and only metal casting operations were recorded; they do not form part of research presented here.

3. Materials and methods

The analysis of an initial assemblage of nine copper-based slags was conducted at the Wolfson Laboratories of Archaeological Science of the Institute of Archaeology of UCL, London (**Table 1**). These materials were sampled from a larger collection (estimated c. 20 kg, which include slags, crucibles, casting debris and finished metal artefacts), hosted at the A.Kh. Margulan Institute of Archaeology in Almaty (Kazakhstan). Analyses of additional samples from this collection are currently being carried out at the Institute of Archaeology of UCL, London as part of the PhD research of the lead author. The materials presented here weigh from 3 to 41 g. Samples are labelled as BAE 29-35, and present small differences in macroscopic appearances. Sample BAE 29 is a dark fragment exhibiting a flow-like shape and a vitrified surface, small bloating voids on both sides and green and reddish patches; it tested as magnetic. Samples BAE 40 and BAE 45 are brown in colour with green patches on the surface and have a flat and rather thin profile. BAE 40 has clearly defined bubble imprints on one side and also tested as magnetic. Samples BAE 30-35 are brown to black slags with amorphous to elongated shape, characterised by numerous bloating voids and vitrified areas. Red and green patches typical of copper and iron oxides are quite common on their surface (**Figure** 7).

Based on the context, samples BAE 29, BAE 30, BAE 40 and BAE 45 were unearthed in the Petrovka layers of the northern complex, sample BAE 32 in the Excavation 3, and the rest of the slags was collected in the eastern complex (**Table 1**), where Petrovka and Alakul-Fedorovo cultural horizons are mixed up. Judging by this, samples BAE 29, BAE 30, BAE 40 and BAE 45 would be dated from 1900 BC - 1800 BC (Petrovka), while samples BAE 31, BAE 32, BAE 33, BAE 34, BAE 35 have a broader life span of c. 200 years, until 1600 BC.

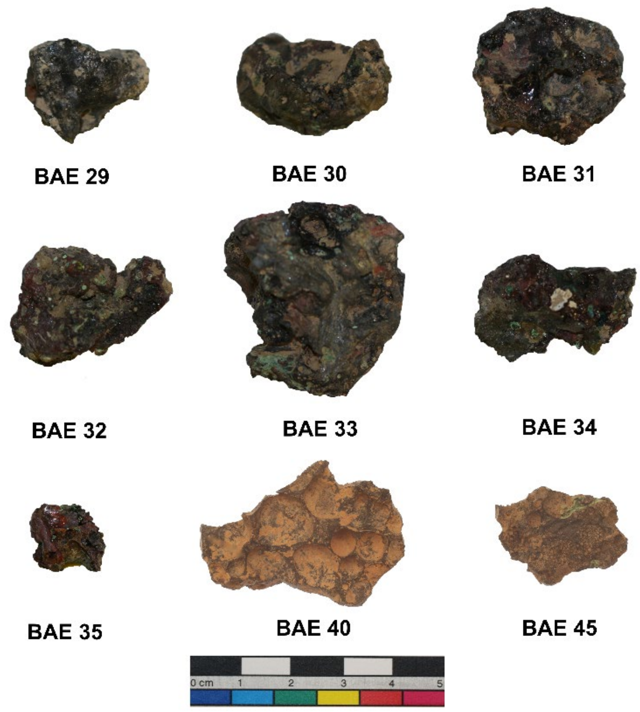

Fig. 7. Copper slags from Taldysai analysed in this study.

Table 1
Analysed metallurgical debris from Taldysai with contextual information.

Label	Expedition	N. of finds	Sample selected for analysis	Excavation	Sector	Square	Depth
BAE 29	2014	2 (a,b)	a	1	Northern com.	E16	70-80 cm
BAE 30	2014	1		1	Northern com.	E16	20 cm
BAE 31	1998	1		1	Eastern com.	B7	20cm
BAE 32	2008	3 (a,b,c)	b	3			30-60 cm
BAE 33	2005	1		1	Eastern com.	Z10	
BAE 34	2008	2 (a,b)	a	1	Eastern com.	Z10	
BAE 35	2007	1		1	Eastern com.	Z10-Z11	
BAE 40	2015	1		1	Northern com.	V17	
BAE 45	2015	1		1	Northern com.	D16	

Materials were first tested with a magnet and cut along the centre with a circular saw and mounted in epoxy resin. Resin blocks were ground and then polished with diamond paste down to 1μm; then, samples were observed for microstructure under Reflected-Light Optical Microscopy using a Leica DM4500 Led instrument with a Leica DFC290 HD camera attached to document the microstructures and the compounds optically visible. Specimens were subsequently carbon-coated and analysed for composition and further microstructural considerations by Energy-Dispersive Scanning Electron Microscopy (SEM-EDS). The instrument in use was a Philips XL 30 ESEM Scanning Electron Microscope equipped with an Oxford Instruments INCA Energy Dispersive X-Ray spectrometer. The machine was operated in high vacuum at 20 kV and 10 mm working distance, and detection limit at around 0.1 wt%. Two to four bulk spectra were collected per sample at 100x magnification (area analyses of slag matrix/glass depleted or with minimal number of inclusions), whereas spot analyses were acquired to characterise single phases. The acquisition time of the spectra was 100 seconds with average dead time of 35-40%. The Certified Reference Material (CRM) for accuracy control was a BHVO-2 basalt standard provided by United States Geological Survey (USGS) (see Appendix, **Table A1**).

Results from compositional analysis were then subjected to different statistical calculations which included Principal Component Analysis (PCA) in R software. Data collected from Taldysai were subsequently analysed against a dataset of metallurgical debris from 2nd millennium BC metalmaking sites/workshops (see **Figure 8** and **Table 2)**. The contributions were selected to include all of the following criteria:

- Material assemblages dated to the 2nd millennium BC (Mid/Late Bronze Age contexts) were analysed;
- Analyses included bulk data of copper smelting slags and/or spot analyses of various phases conducted with SEM-EDS and other accompanying instruments;
- Compositional analyses followed the similar protocol adopted here. This includes presenting all original data for bulk and metallic inclusions as wt%. Normalisation and conversion to FeO and SO_3 from Fe_2O_3, SO and SO_2 were conducted subsequently by the first author to allow consistency.

Fig. 8. Map of Taldysai and the comparative metal production centres detailed in Table 2.

Table 2

Summary information on the reference publications with analysis of copper smelting debris from the 2nd millennium BC contexts in Eurasia.

Site	Region/ District	Chronology	Materials	Analytical protocol								Reference
				OM	XRD	XRF	SEM-EDS	EPMA	ICP-OES	LIA	Bulk for database	
Luserna **(1)**	S-E Alps (Trentino) **(A)**	ca 1500/1400-1200 BC	Cu slags	x	x	x	x	x		x	XRF (pellets)	Addis et al. (2016)
Segonzano **(2)**, Transacqua **(3)**	S-E Alps (Trentino) **(A)**	ca 1500/1400-1200 BC	Cu slags	x	x	x	x	x		x	XRF (pellets)	Addis et al. (2017)
Raxgebiet area **(4)**	N-E Alps **(A)**	1000-900 BC	Cu slags	x		x		x			ED-XRF	Larreina-Garcia et al. (2015)
Politiko Phorades **(5)**	Cyprus **(B)**	ca 1650-1500 BC	Cu slags			x	x				XRF (pellets)	Knapp and Kassianidou (2008)
Supsa-Gubazeuli rivers area **(6)**	S-W Caucasus **(C)**	1500-900 BC	Cu slags	x			x				SEM-EDS	Erb-Satullo et al. (2014)
Supsa-Gubazeuli area rivers **(6)**	S-W Caucasus **(C)**	1500-900 BC	Cu slags on tech. ceramics	x			x				SEM-EDS	Erb-Satullo et al. (2015)
Kamennyi-Ambar **(7)**	S Urals (Russia) **(D)**	2100-2000 BC	Cu slags	x			x	x			SEM-EDS	Zaykov et al. (2013)
Laoniupo **(8)**	Shaanxi (Central China) **(G)**	ca 1415-1295 BC	Cu-/Cu-As slags on tech. ceramics and tech.ceramics	x		x	x				XRF (pellets)	Chen et al. (2017)

Taijiasi **(9)**	Anhui province (N-E China) **(G)**	ca 1350-1300 BC	Cu-slags and tech. ceramics	x	x		x				SEM-EDS	Liu et al. (2020)

4. Results

Copper extraction from sulfidic ores is generally described as a multi-step process (Craddock, 1995); the general aim of these steps is to drive away sulfur and iron, as main components of primary copper ores. During the initial smelting, (copper) sulfides would liquify around 900°C in a reducing atmosphere, and their melting upon separation from a siliceous ore gangue would result in the formation of matte nodules, such as Cu/Cu-Fe sulfides of characteristic grey/blue colour (see example in **Figure 10b-c**). Matte is then further roasted to remove the sulfur and extract copper metal. However, when iron is present in the charge in significant amount (as it is in primary copper ores such as chalcopyrite), the obtained matte would need to undergo a further smelting step with a flux (e.g. silica), which will bond with iron to produce slag, usually rich in fayalite (Koucky and Steinberg, 1982, Bachmann, 1982, Craddock 1995). In this way, initial steps would aim at driving off the sulfur, while the rest would deal with removing the iron (ideally through slagging) (Killick, 2014). Depending on the ore, different silica or iron oxide concentrations may be naturally present in the charge as gangue material, which may act as a flux.

Variations to this understanding include co-smelting of copper oxides/carbonates and copper sulfides (primary) (Rostoker et al., 1989). The co-smelting of Cu oxides (carbonates) and sulfides must have taken place early on in the evolution of metallurgy, assuming that the secondary copper ore sources were relatively quickly exploited (Rostoker et al., 1989; Killick, 2014; Bourgarit, 2007). This has been experimentally reproduced by Rostoker et al. (1989), who proposed the following reaction:

[1] $2Cu_2S + 3O_2 \rightarrow 2Cu_2O + 2SO_2$
[2] $Cu_2S + 2Cu_2O \rightarrow 6Cu + SO_2$

in which [1] describes the oxidation of Cu_2S (chalcocite) into cuprous oxide (Cu_2O) and a consequent release of sulfur dioxide. The cuprous oxide then keeps the reaction with Cu_2S further added to the charge [2] to produce metallic copper and emits additional sulfur dioxide. We have examined metallurgical debris from Taldysai in the light of the processes already known to archaeometallurgical scholarship.

Compositional and microstructural analyses of Taldysai slag identified two macro groups. One includes 6 slags and is related to pure copper production (type T1a). The other includes samples with arsenical copper smelting evidence and has two sub-types: T1b (samples BAE 40 and BAE 45) and T2b (sample BAE 29). The decision to create these three sub-types was based on the number of steps required for each production line (copper and arsenical copper respectively): T1a refers to the single (co-)smelting step to obtain copper, while T1b and T2b demonstrate two-step production. In further text we shall refer to copper production line as ‘a’ and arsenical copper production as ‘b’.

Table 3
SEM-EDS bulk composition of slags from Taldysai. Data normalised to 100% and expressed as wt%. SD = Standard Deviation. Bdl = Beyond Detection Limit. The FeO in samples BAE 29, BAE 40 and BAE 45 is quantified as FeO^t.

Sample	Measures	Na_2O	MgO	Al_2O_3	SiO_2	P_2O_5	SO_3	K_2O	CaO	Sc_2O_3	TiO_2	MnO	FeO	CoO	CuO	As2O3	SrO	BaO
Slag type T1a																		
BAE 30 average	3	**1.9**	**0.8**	**25.9**	**47.7**	**bdl**	**bdl**	**4.2**	**0.5**	**bdl**	**0.8**	**bdl**	**8.3**	**bdl**	**9.9**	**bdl**	**bdl**	**bdl**
SD		0.9	0.3	5.1	2.4	-	-	1.6	0.3	-	0.5	-	4.1	-	3.0	-	-	-
BAE 31 average	3	**2.5**	**1**	**17.9**	**49.3**	**1.8**	**bdl**	**2.3**	**5.8**	**bdl**	**0.6**	**0.3**	**12.6**	**bdl**	**5.9**	**bdl**	**bdl**	**bdl**
SD		0.5	0.3	0.6	6.0	1.0	-	0.2	3.5	-	0.1	0.0	2.2	-	1.3	-	-	-
BAE 32 average	3	**1.8**	**0.5**	**16.1**	**43.4**	**0.5**	**0.3**	**2.6**	**3.3**	**bdl**	**0.5**	**bdl**	**4.0**	**bdl**	**26.8**	**bdl**	**bdl**	**bdl**
SD		0.1	0.3	2.1	5.1	0.9	0.1	1.6	2.0	-	0.1	-	0.8	-	13.1	-	-	-

BAE 33 average	3	**2.8**	**1.1**	**19.6**	**53.6**	**0.9**	**bdl**	**2.9**	**4.0**	**bdl**	**0.7**	**bdl**	**10.6**	**bdl**	**3.8**	**bdl**	**bdl**	**bdl**
SD		0.3	0.3	1	6.4	0.9	-	0.4	2.8	-	0.1	-	1.7	-	1	-	-	-
BAE 34 average	3	**3.1**	**0.2**	**17.4**	**56.8**	**1.1**	**0.9**	**3.7**	**0.8**	**bdl**	**0.6**	**bdl**	**8.3**	**bdl**	**6.9**	**bdl**	**bdl**	**bdl**
SD		0.3	0.0	1.3	4.0	1	0.3	1	0.4	-	0.1	-	3.1	-	0.4	-	-	-
BAE 35 average	4	**2.9**	**0.7**	**15.8**	**55.6**	**1.0**	**bdl**	**2.8**	**3.4**	**bdl**	**0.5**	**bdl**	**6.6**	**bdl**	**10.7**	**bdl**	**bdl**	**bdl**
SD		0.7	0.3	3.3	3.3	0.8	-	0.7	2.4	-	0.1	-	1.0	-	3.9	-	-	-
Slag type T1b																		
BAE 40 average	3	**2.0**	**3.9**	**9.3**	**40.1**	**1.0**	**0.0**	**2.0**	**12.7**	**0.1**	**0.5**	**0.1**	**26.8**	**0.1**	**0.7**	**bdl**	**0.5**	**bdl**
SD		0.2	0.1	0.2	0.3	0.0	0.0	0.1	0.2	0.0	0.0	0.0	0.3	0.1	0.2	-	0.1	-
BAE 45 average	2	**2.1**	**1.1**	**6.4**	**37.4**	**0.6**	**0.0**	**0.8**	**11.0**	**bdl**	**0.2**	**0.0**	**34.8**	**bdl**	**3.6**	**1.2**	**0.5**	**0.1**
SD		0.2	0.0	0.2	0.1	0.1	0.0	0.0	0.1	-	0.1	0.0	2.3	-	3.3	0.5	0.1	0.1
Slag type T2b																		
BAE 29 average	2	**1.7**	**0.4**	**8.1**	**19.3**	**bdl**	**bdl**	**0.6**	**1.5**	**bdl**	**1.6**	**0.5**	**66.2**	**bdl**	**0.2**	**bdl**	**bdl**	**bdl**
SD		0.5	0.1	1.1	2.5	-	-	0.4	0.7	-	1.5	0.1	4.6	-	0.3	-	-	-

Table 4

Newly formed mineral and metallic phases detected in slag types T1a, T1b and T2b from Taldysai.

Mineral phases	**Slag type**		
	T1a	**T1b**	**T2b**
Oxides			
Wüstite (FeO)			x
Magnetite (Fe_3O_4)		x	x
Delafossite ($CuFeO_2$)	x		x
Cuprite (Cu_2O)	x		
Silicates			
Hedenbergite ($CaFeSi_2O_6$)		x	
Augite $(Ca,Na)(Mg,Fe,Al,Ti)(Si,Al)_2O_6$		x	
Fayalite (Fe_2SiO_4)		x	x
Quartz (SiO_2)	x	x	
Metallic phases			
Pure Cu metallic phases	x		
Cu-As metallic phases		x	x
Fe-Cu-As speiss		x	
γ phases (Cu_3As)		x	

4.1. Slag type T1a

This first type of slags is dominated by silica and alumina (on average 51 wt% and 18 wt% respectively) (**Table 3**). The texture features bloating holes and fully liquified slag matrix in which oxides, copper metallic prills and sulfidic inclusions are embedded (**Figure 9**). Copper oxide constitutes the third main bulk component of these slags, both in the form of copper metal and "dross", recorded almost up to 30 wt% in the bulk (sample BAE 32 and **Table 3**). Copper and copper-iron oxides such as cuprite (Cu_2O) and delafossite ($Cu^{+}Fe^{+3}O_2$) were spotted in these samples, which generally indicate borderline oxidising conditions in which it was possible to extract copper metal (Bachmann, 1982; Hauptmann, 2000; Bourgarit, 2007; Chen et al., 2017; Radivojević et al., 2010; Radivojević, 2013) (**Table 4**).

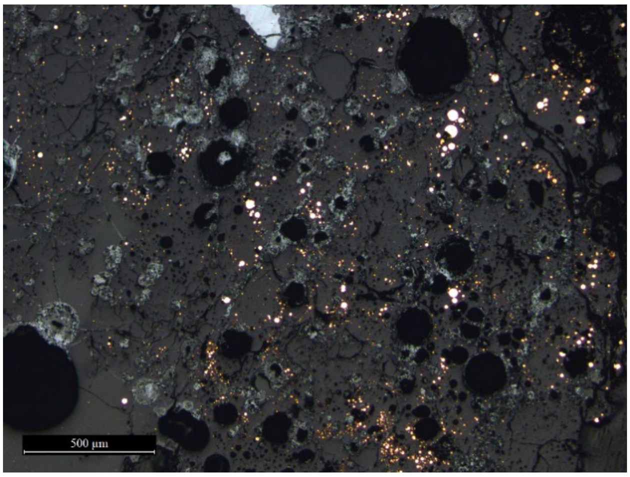

Fig. 9. Photomicrograph of BAE 30 reporting an example of the bloated and vitrified matrix of the T1a slags, taken under plane polarised light (50x magnification). Abundant copper metal prills are visible as shiny/orange-coloured inclusions, alongside numerous newly formed chalcocite and copper oxides phases (paler and darker grey).

Sulfides in these slags are represented with chalcopyrite ($CuFeS_2$), bornite (Cu_5FeS_4), chalcocite (Cu_2S) and covellite (CuS). A single grain of chalcopyrite was observed as yellow, sub-angular and partially reacted, decomposed into pink bornite lamellae and blue chalcocite. It also included small copper metal phases (**Figure 10a**) and traces of Ag (0.3 wt% and **Table A2** in Appendix). Previous analyses by Artemyev and Ankushev (2019) and Ankushev et al. (2021)suggested that relatively high levels of silver in sulfidic inclusions represent specific marker of the use of cuprous sandstone in slags from Taldysai, but also in slags from the Late Bronze Age sites of the Cis-Urals (Ordinsky Ovrag, Tokskoe, Ivanovskoe, Bulanovskoe 2, Pokrovskoe, Rodnikovoe, Kuzminkovskoe 2). In the Late Bronze Age Srubnaya cultural horizons in the Cis-Urals, slags comparable in composition, microstructure and phases to these at Taldysai exhibited Cu sulfides phases with trace silver quantified in tens of ppm (Artemyev and Ankushev, 2019: 18). Slags T1a also present chalcocite as newly formed phases, which are characterised as sub-spherical matte (**Figure 10b**) enclosing copper metal prills (**Figure 10c**). All metal prills in T1a slags are made of unalloyed high purity copper metal, except for low Fe and sulfur contents (**Table 5**), which would not be unusual for copper metal extraction with this quality of ores (Bachmann, 1982; Craddock and Meeks, 1987). In Southern Urals, the exploitation of cuprous sandstone for extracting pure copper metal is also documented at the Late Bronze Age site of Gorny in the Kargaly mining district (Rovira, 1999; Chernykh, 2004). Bulk composition, microstructure, and phases of T1a slags from Taldysai find close comparison with those documented at Gorny (Rovira, 1999: 96, Figure 6:A; Chernykh, 2004: 109, Figure 4.2:6). Noteworthy, slags obtained through experimental smelting of the cuprous sandstone from the Kargaly ore field yielded smelting debris comparable to the archaeological examples unearthed at Gorny (Rovira, 1999: 104-108). Similar examples were produced after the experimental smelt in Taldysai, using a charge that included secondary sulfides (chalcocite) from the Dzhezkazgan area (Calgaro and Radivojević, 2022). At Gorny, experimental smelting was carried out both in holes in the ground and in above-ground furnaces made of sandstone rocks using up to three bellows. In contrast, experimental smelting at Taldysai used a replica of the archaeological vaulted pit furnace as shown in **Figure 4** without any forced blast (Artyuhova et al., 2013; Yermolayeva and Rusanov, 2022). The results of experimental slags analysis are highly identical with the slag type T1a from Taldysai, hence further reinforcing the argument that Taldysai metallurgists exploited sulfidic ores from the secondary horizon of mineralisation, such as chalcocite (Cu_2S) and bornite (Cu_5FeS_4), but most likely also copper oxides, carbonates and sulfates (which included cuprite (Cu_2O), tenorite (CuO), azurite ($C_2H_2Cu_3O_8$), malachite ($Cu_2CO_3(OH)_2$), brochantite $Cu_4SO_4(OH)_6$), from the contact upper horizon of Dzhezkazgan mineralisation. Hence, these ores would undergo a co-smelting process to extract copper metal. In support of this, abundant fragments of copper oxides, carbonates and sulfates with the above-mentioned composition have been found in all areas of the settlement and are currently subject of analysis at the UCL Institute of Archaeology.

In T1a slags from Taldysai analysed so far within the doctoral project of the first author and by Ankushev et al. (2020), primary chalcopyrite is absent, if not for the unreduced inclusion we report in **Figure 10a** and another spare inclusion reported by Artemyev and Ankushev (2019: 9, Figure 2h). Based on this and considered the average low FeO recorded in T1a slags (**Table 3**), we propose that chalcopyrite was in sporadic use, if any, and that the main charge was cuprous sandstone, which here stands for a mix of copper oxides and secondary sulfides and silica, low in iron oxides. This type of ore is local to Dzhezkazgan, which makes it the most likely candidate, even in the absence of provenance analysis.

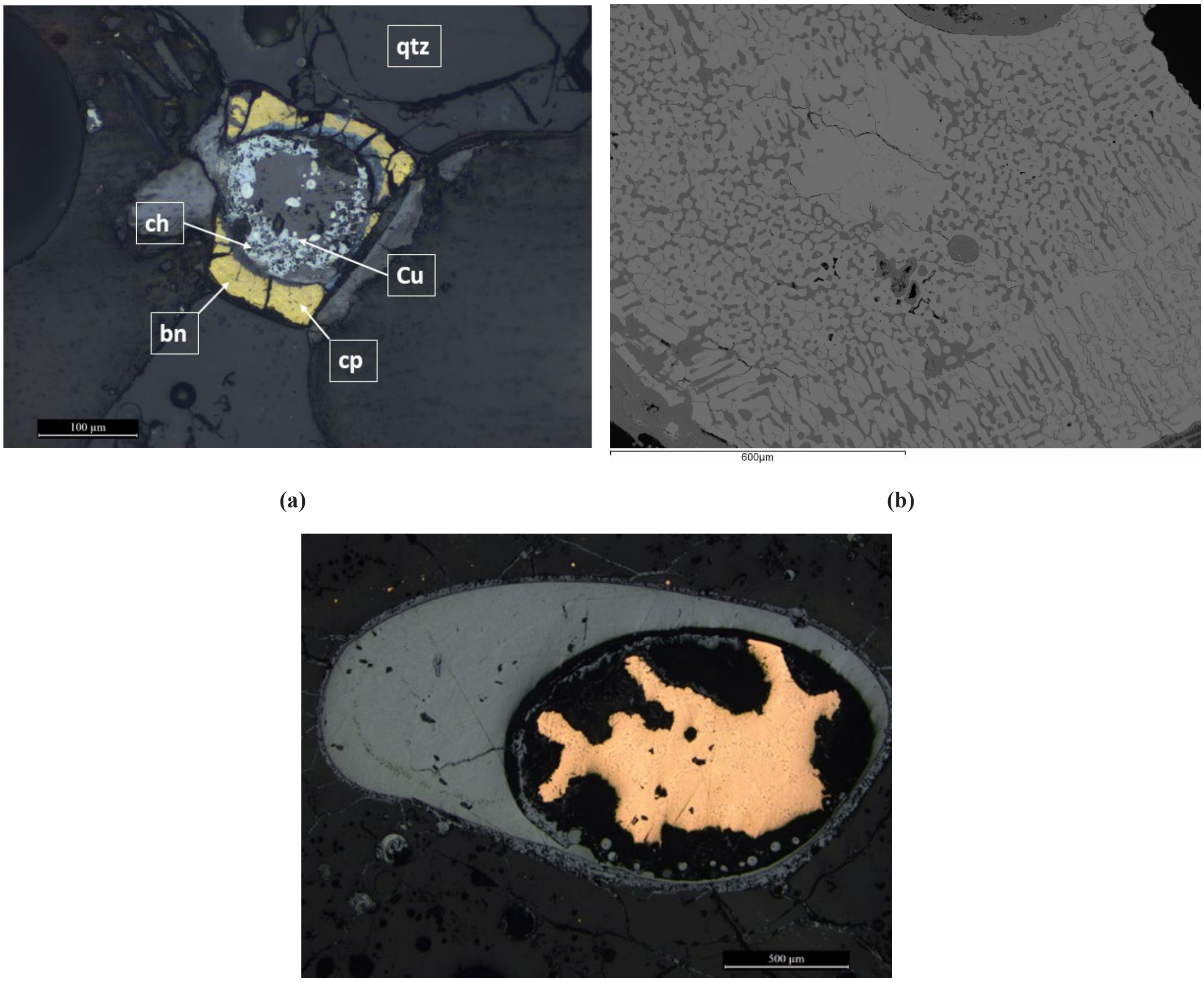

(a) (b)

(c)

Fig. 10. (a) Photomicrograph of chalcopyrite (cp) inclusion with bornite (bn) lamellae, chalcocite (ch) and a tiny copper metal prill (Cu). A grain of thermally reacted quartz (qtz) stands at the top (sample BAE 35, PPL, mag. 200x). (b) SEM-EDS BSE image showing a partially reduced matte inclusion. Note the colour contrast between chalcocite (paler) and copper oxide (darker) (sample BAE 33). (c) Photomicrograph showing pale blue chalcocite surrounding a copper metal droplet (shiny/orange) (sample BAE 31, PPL, mag. 100x).

4.2. Slag type T1b

This slags group is abundant in silica (c. 37-40 wt%), and lower in alumina than group T1a (c. 6-9 wt%), but higher in FeO content (up to 34 wt%). Soda, magnesia and phosphate readings are comparable to those in group T1a, whereas the lime content is strikingly higher here, reaching up to 12 wt% (**Table 3**). This is reflected in the mineralogy of these samples, as the surface alternates large intergrowths of fayalite (Fe_2SiO_4) to Ca-rich pyroxene phases, such as hedenbergite ($CaFeSi_2O_6$), augite (Ca,Na)(Mg,Fe,Al,Ti) (Si, Al)$_2$O$_6$ and other silica-calcium rich phases (**Figure 11**). These mineral phases are characterised by traces of vanadium, chromium, cobalt, nickel and antimony, which were not observed in slags T1a (see Appendix, **Tables A7-A12**). In our case, fayalitic olivine exhibits elongated chain texture (**Figure 11b**). The crystallisation habitus of mineral phases such as olivine is often used to estimate the cooling rate of slag materials (Addis et al., 2016; 2017; Bourgarit, 2019: 221; Hauptmann, 2020). According to Donaldson (1976: 199) the chain habitus (as in **Figure 11b**) reflects a fast crystallisation rate occurring between 80 °C/hr - 350 °C/hr . On the other hand, polyhedral lathes (‘hopper habitus’) usually mirror slower cooling rates (0.5 ºC/h to 40 °C/h, also below). Subhedral spinels aggregates, such as magnetite (Fe_3O_4), are also present, suggesting that T1b slags presumably formed in a mildly oxidised atmosphere (**Figure 11a; c**). The bulk CuO content does not exceed 3 wt% in these slags, and traces of scandium, cobalt, strontium and barium are noticed (**Table 3**).

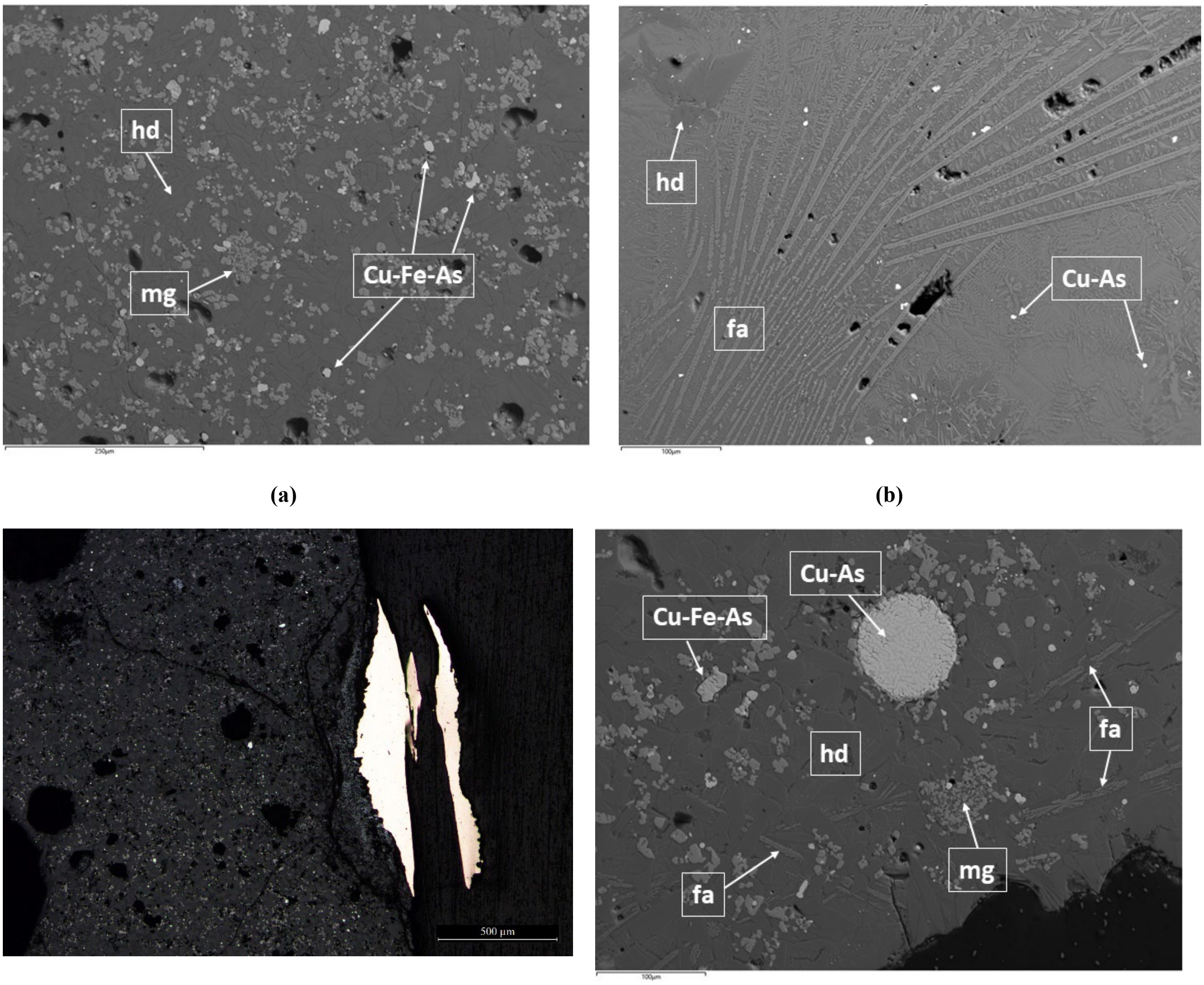

(a) (b)

(c) (d)

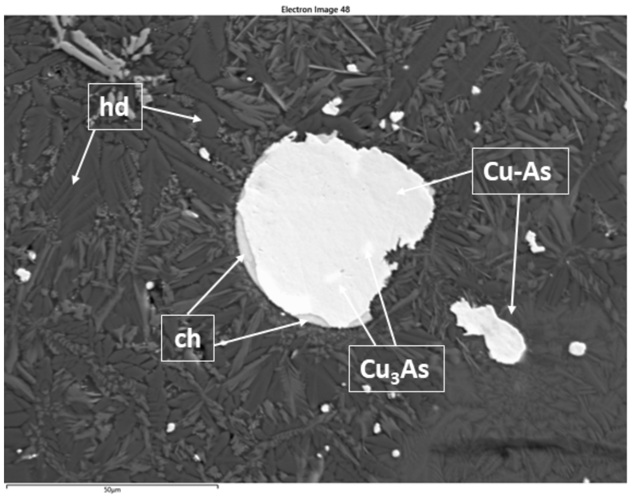

(e)

Fig. 11. (a) SEM-EDS BSE image of hedenbergite (hd) lathes, magnetite (mg) aggregates and Cu-As prills (sample BAE 45). (b) SEM-EDS BSE image of a well-formed intergrowth of chain fayalite (fa) between hedenbergite (hd) phases on the up left and other feathery Ca-rich phases on the right (mid-grey). Shiny Cu-As prills are widely scattered in matrix (sample BAE 40). (c) Photomicrograph of the exposed surface of a large Cu-As prill embedded in slag matrix (sample BAE 45, PPL, mag. 50x). (d) SEM-EDS BSE image of dark blocky lathes of hedenbergite (hd) alongside magnetite (mg) clusters, chain fayalite (fa), mid-grey metallic inclusions with Cu-Fe-As composition (speiss) and Cu-As prills, the largest of which shows a biphasic appearance due to partial corrosion (sample BAE 45). (e) SEM-EDS BSE image of a Cu-As prill with light γ-phases (Cu_3As, the arsenic content is around 30 wt%, whereas the 'darker' portion of metal matrix is about 8 wt%, see Table 5). The pale grey borders of the prill are chalcocite (ch) rims with low concentrations of iron and selenium (see Appendix, Tables A3 and A4). On the background are dark hedenbergite (hd) and paler silica-lime-rich phases (sample BAE 40).

In contrast to slags T1a, metallic prills (up to 1 mm in diameter, **Figure 11c**) in T1b are made of arsenical copper, with arsenic content ranging from a minimum of ca 3-5 wt% to a maximum of about 30 wt% in bright white γ-phases (**Figure 11d** and **Table 5**). Metal prills are evenly scattered in the matrix of these slags and at times present sulfidic rims with chalcocite composition and small quantities of iron and selenium (**Figure 11d** and Appendix, **Tables A3, A4**), in line with previous analyses on flat-type slags from Taldysai carried out by Ankushev et al. (2020). In addition, inclusions of copper-rich 'speiss' (Bachmann, 1982; Thornton et al., 2009; Rehren et al., 2012), with Fe between 6-20 wt%, As between 27-33 wt% and trace readings of cobalt, nickel, selenium and sulfur were noticed (mid-grey in **Figure 11a; d** and reported in Appendix, **Tables A5-A6**). The above observations point to the use of iron and arsenic-rich ores in the smelting, the nature of which is still to be confirmed. Multiple options could fit this production line:

The first option *(i)* entails the co-smelting of local chalcocite and bornite with copper arsenates such as lammerite ($Cu_3(AsO_4)_2$) and olivenite (Cu_2AsO_4OH) or the co-smelting of copper arsenates with copper metal (e.g. as documented at Chalcolithic Çamlibel Tarlası by Boscher, 2016; Rehren and Radivojević, 2010). Cu arsenates have typical green hue and can be geologically associated with copper-bearing minerals such as malachite, azurite, tennantite and chalcopyrite (Stöllner, 2018: 96). Outcrops of copper arsenates are not listed among present-day minerals of Dzhezkazgan, even though it is not to exclude that they might have been present in antiquity. However, the co-smelting of copper arsenates with either secondary Cu and Cu-Fe sulfides or with copper metal, regardless the presence of speiss phases, would not explain lathes of fayalite and abundant spinels in T1b, which rather suggest *(a)* slagging of an iron-rich ore or simply that *(b)* this smelting charge was relatively iron rich. As we saw for T1a slags, the iron content of secondary sulfides solely does not justify such iron levels.

(ii) Tennantite ($Cu_6(Cu_4Fe^{2+}_2)As_4S_{12}S$), a copper sulfarsenide, is reported in the high depth primary mineralisation horizon of Dzhezkazgan, and so was *(iii)* arsenopyrite (FeAsS), an iron sulfarsenides, likely in association with its weathered by-product scorodite ($FeAsO_4·2H_2O$) (above, Satpaeva, 2007; Ankushev et al., 2020). These could have been co-smelted with copper oxides/carbonates or with copper sulfides such as chalcocite and bornite sourced in the Dzhezkazgan, i.e. the source for pure copper metal (T1a). It is unknown whether these deposits were exploited during the Bronze Age, even though, given the complex stratiform nature of mineral deposits of the area, this scenario cannot be excluded. Because both iron and arsenic are present in these three minerals, they represent good candidates for the arsenical copper production line and T1b slags (Merkel and Shimada, 1988; Lechtman and Klein, 1999). The presence of matte in T1b slags implies

that sulfides were also part of the charge, which again goes well with the use of tennantite or arsenopyrite/scorodite ores. Noteworthy, Lechtman and Klein (1999: 498-499) report that when co-smelting a charge of copper or iron sulfarsenides and copper oxides, the sulfur in the ore charge would oxidise being a reducing agent and volatise as sulfur dioxide, leaving behind a CuAs alloy if using copper sulfarsenides or CuAs and FeO when using iron sulfarsenides, plus a series of by-products, such as matte and speiss. This scenario would eliminate the roasting step (to get rid of the sulfur), hence the possibility of losing arsenic in form of poisonous gas, which could have caused significant health damage for metalsmiths. Fluxes such as silica or iron oxides/hydroxides could have been added to the smelting charge to help the formation of slags and such veins are mineralised alongside copper ores in Dzhezkazgan. Lechtman and Klein (1999) did not use any fluxes when experimentally co-smelting copper oxides and the copper sulfarsenide enargite (Cu_3AsS_4) in a bowl-furnace at temperatures reaching 1150°-1200°C. In this experiment, the intake of fuel acting as a flux would be high in the slags (20 wt% CaO), which does not correlate with the readings from **Table 3**.

At this stage, we cannot completely rule out that *(iv)* speiss could have been produced separately and then added to copper metal as proposed by Rehren et al. (2012). Based on our evidence, all analysed T1b and T2b (below) slags are found to contain copper, including arsenical copper slags analysed by Ankushev et al. (2020). This is in contrast to the 'speiss slags' documented at the Early Bronze Age sites of Arisman and Tepe Hissar (Thornton et al., 2009; Rehren et al., 2012). Forthcoming analyses of the already sampled materials included in the first author's doctoral project will contribute to further clarifications on this matter.

Considering the thin profile and the bubbly macroscopic appearance of one of the samples (BAE 40, Figure 7), it is likely that T1b slags formed as the top layer of a smelting charge. This could have taken place within a crucible in bowl-shaped above-ground furnaces at Taldysai, as proposed also by Ankushev et al. (2020). In this respect, note that Thornton et al. (2009: 312) suggested that relatively high calcium level in one of their speiss slags from Early Bronze Age Tepe Hissar was due to a fragment of furnace or crucible lining entrapped in one of those slags (about 11 wt%, Thornton et al., 2009: 311, Table 1). A similar calcium concentration was reported also by Rehren et al. (2012: 1721, Table 4, between 14-19 wt%; 1725) and interpreted as interaction with technical ceramics for the speiss slags from the Early Bronze Age site of Arisman. Noteworthy, crucible vessels have been unearthed at Taldysai nearby smelting installations (A.S. Yermolayeva, pers. comm.). They show evidence for vitrification and characteristic red and green patches usually related to (s)melting operations and form part of the collection currently under investigation at the UCL Institute of Archaeology to better understand their role in metal production.

4.3. Slag type T2b

This type is represented with slag sample BAE 29. It stands out for significantly higher FeO content, 66 wt% on average, and association with traces of MnO (up to 0.5 wt%) (**Table 3**). Iron oxides dominate the chemistry of this sample in form of long white dendrites of wüstite (FeO), a strong indicator of reducing conditions, and aggregates of spinels as magnetite (**Figure 12a, Table 4**). The composition of spinels includes both Fe^{+2} and Fe^{+3}, implying a formation in environments with intermediate oxygen levels and, consequently, in more oxidising conditions than FeO. As such, their concentration on one side of the sample would suggest that this portion of BAE 29 (the surface, presumably) underwent sudden exposure to oxidation, as highlighted by the large voids and by the presence of delafossite associated with magnetite (**Figure 12b**), hence that the redox conditions within the furnace or crucible were highly variable. Fayalitic olivine alternates the chain (**Figure 12a**) to the hopper habitus (**Figure 12b**), which points to an average slow cooling rate of this slag and seemingly suggests that this slag was broken while still hot (cf. Pearce et al., 2022).

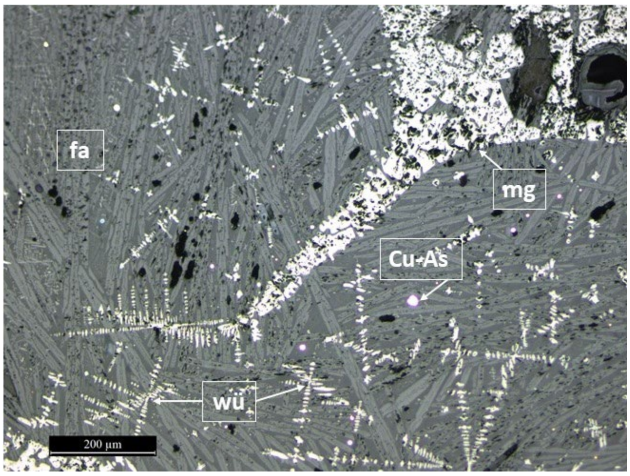

(a)

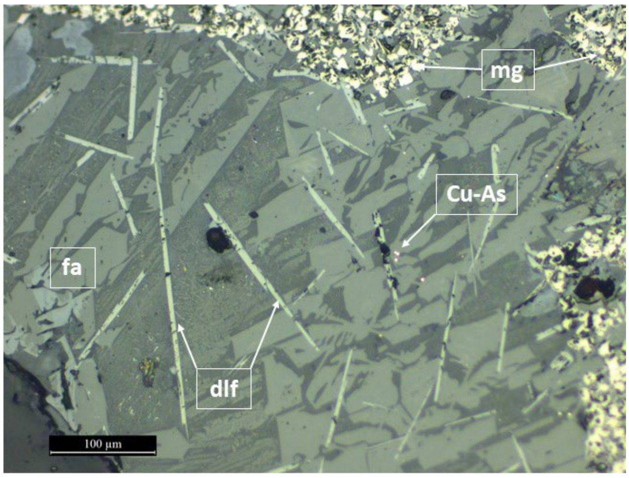

(b)

Fig. 12. (a) Photomicrograph of sample BAE 29 showing white dendrites of wüstite (wü) and magnetite clusters (mg, white) over elongated chain fayalite (fa, pale grey) in a glassy matrix (dark interstitial grey). Small shiny Cu-As metallic prills are scattered in the matrix (PPL, mag. 100x). (b) Micrograph showing platy delafossite (dlf) lathes over hopper fayalite (fa) and feathery glassy matrix; subhedral magnetite (mg) distributes on the borders of the micrograph, while tiny metallic prills (Cu-As) are visible in the centre (PPL, mag. 200x).

Only few copper metal prills containing relevant arsenic readings (up to 8 wt%), while low Fe and Ni were detected in this specimen (up to 2 and 0.8 wt%, respectively) as in metallic prills of slags T1b, which indicates that they may have been obtained out of the same type of arsenic and iron-rich ores observed in group T1b, or they possibly represent a further processing of the matte production likely carried out in crucibles (**Table 5**). In support of this, sulfidic phases are absent here.

Table 5
SEM-EDS compositional values of metallic prills detected in samples BAE 29-45. Data normalised to 100% and expressed as wt%; SD = Standard Deviation.

Sample	Measures		O	S	Fe	Co	Ni	Cu	As	Se	Ag
Slag type **T1a**											
BAE 30	8	Min	0.3	bdl	0.0	bdl	bdl	96.6	bdl	bdl	bdl
		Average	**0.4**	**-**	**0.4**	**-**	**-**	**99.1**	**-**	**-**	**-**
		Max	0.6	bdl	3	bdl	bdl	99.6	bdl	bdl	bdl
		SD	0.1	-	1.1	-	-	1	-	-	-

BAE 31	4	Min	0.4	0.0	0.0	bdl	bdl	98.1	bdl	bdl	bdl
		Average	**0.5**	**0.9**	**0.1**	**-**	**-**	**98.5**	**-**	**-**	**-**
		Max	0.6	1.2	0.3	bdl	bdl	99.1	bdl	bdl	bdl
		SD	0.1	0.6	0.1	-	-	0.4	-	-	-
BAE 32	1		bdl	1.5	bdl	bdl	bdl	98.5	bdl	bdl	bdl
BAE 33	3	Min	0.4	0.0	0.0	bdl	bdl	97.8	bdl	bdl	bdl
		Average	**0.5**	**0.7**	**0.2**	**-**	**-**	**98.5**	**-**	**-**	**-**
		Max	0.6	1.1	0.4	bdl	bdl	99.6	bdl	bdl	bdl
		SD	0.1	0.6	0.2	-	-	1	-	-	-
BAE 34	3	Min	0.5	0.0	0.0	bdl	bdl	96.5	bdl	bdl	bdl
		Average	**0.6**	**1.2**	**0.5**	**-**	**-**	**97.7**	**-**	**-**	**-**
		Max	0.7	2.4	1	bdl	bdl	98.4	bdl	bdl	bdl
		SD	0.1	1.2	0.5	-	-	1	-	-	-
BAE 35	5	Min	0.6	0.0	0.0	bdl	bdl	98	bdl	bdl	bdl
		Average	**0.8**	**0.3**	**0.1**	**-**	**-**	**98.8**	**-**	**-**	**-**
		Max	1	0.8	0.8	bdl	bdl	99.2	bdl	bdl	bdl
		SD	0.4	0.3	0.4		-	0.5	-	-	-
Slag type **T1b**											
BAE 40 **arsenic-poor phase**	12	Min	0.4	bdl	bdl	bdl	bdl	87.1	0.5	bdl	bdl
		Average	**0.8**	**0.0**	**2.1**	**0.0**	**-**	**91.0**	**6.4**	-	0.0
		Max	2.5	0.0	4.1	0.0	bdl	97.8	10.2	bdl	0.0
		SD	0.6	-	1.4	-	-	2.6	2.9	-	-
BAE 40 arsenic-rich phase	2	Min	0.4	0.0	0.6	bdl	bdl	68.3	29.4	bdl	bdl
		Average	**0.4**	**0.0**	**1.3**	**-**	**bdl**	**68.8**	**29.5**	**-**	**-**
		Max	0.4	0.0	1.9	bdl	bdl	69.4	29.5	bdl	bdl
		SD	0.0	0.0	0.9	-	-	0.8	0.1	-	-
BAE 45 arsenic-poor phase	3	Min	0.4	bdl	0.0	bdl	bdl	94.9	2.8	bdl	bdl
		Average	**0.5**	**-**	**0.0**	**-**	**-**	**96.1**	**3.4**	**-**	**-**
		Max	0.5	bdl	0.1	bdl	bdl	96.7	4.4	0.0	bdl
		SD	0.0	-	0.1	-	-	1.0	0.9	-	-
BAE 45 arsenic-rich phase	9	Min	0.5	0.2	0.2	bdl	bdl	64.0	21.1	bdl	bdl
		Average	**1.2**	**0.3**	**1.6**	**-**	**-**	**69.1**	**29.2**	**-**	**-**
		Max	4.7	0.7	4.1	bdl	0.1	73.2	32.1	bdl	0.0
		SD	1.4	0.2	1.3	-	0.0	2.7	3.1	-	-
Slag type **T2b**											
BAE 29	2	Min	0.5	bdl	2	bdl	0.4	88.5	7.7	bdl	bdl
		Average	**0.5**	**-**	**2.2**	**-**	**0.6**	**88.7**	**8.0**	**-**	**-**

		Max	0.6	0.0	2.4	bdl	0.8	88.9	8.3	bdl	bdl
		SD	0.1	-	0.3	-	0.3	0.3	0.4	-	-

4.4 Metal smelting technology at Taldysai

The chemistry of metallurgical debris is a function of the interaction of ore, clay (from the furnace lining or ceramic reaction vessel), flux(es) and fuel ash. Hence, slag components are present in different concentrations as a result of the quality of raw materials, redox conditions, skills, design of the smelting installation and similar. In **Table 6** we present which compounds detected in the studied slags may have derived from which slag component (fuels/clays/ores). Some of the oxides in slags may have multiple origin. For example, ores presenting high quantities of siliceous gangue may require the use of a Fe or Mn-rich ore as a flux to form a siliceous slag. On the other hand, the smelting of copper ores rich in iron such as Cu-Fe sulfides would use silica (quarzitic sand) to improve the separation of iron from copper metal and form a fayalitic slag (Addis et al., 2016; Hauptmann, 2020). As mentioned in Section 2, copper-rich ores of Dzhezkazgan are mineralised within both silica gangue material, but also iron oxides and hydroxides.

Table 6

Parent components contributing to the copper slag chemistry. Lime is listed as a fuel ash component, though it might result from the ore charge when smelting so-called self-fluxing ores. Silica and alumina are considered both clay/flux and ore.

	Na_2O	MgO	SiO_2	Al_2O_3	P_2O_5	SO_3	K_2O	CaO	Sc_2O_3	TiO_2	MnO	FeO	NiO	CoO	CuO	As_2O_3	SrO	BaO
Fuel ash	X	X			X		X	X										
Clay			X	X				X		X							X	
Ore//flux			X	X		X		X	X		X	X	X	X	X	X	X	X

The PCA performed on bulk values of slags T1a, T1b and T2b underlines the differences discussed above and related to their composition and mineralogy (**Figure 13**). The PC1 axis defines a neat clustering of the T1a scores (copper metal smelting) alongside the angle defined by Al_2O_3, K_2O, CuO SO_3 and SiO_2 vectors. T1a slags plot closely, which is expected - considering their roughly similar composition. The CuO vector is aligned with the high concentration of copper metal and oxides in T1a slags, whereas SO_3 accounts for the high volume of sulfidic inclusions in these. On the other hand, T1b slags (arsenical copper smelting) are on average more impacted by higher lime content (likely related to their formation in crucible vessels) and additional variance, which derives from the distinctive ore signatures of arsenic, cobalt, barium and scandium. These likely speak of the use of, at least partly, different smelting charges than T1a slags.

As for the T2b slag (arsenical copper smelting), this positively correlates with T1b slags, although it plots on its own due to the high FeO content and the MnO trace readings (**Table 3**). We interpret this as a further stage of production after the step producing the matte and the Cu-As prills in T1b slags, in which the surplus iron remained upon matting is released in the slag matrix during matte smelting and ends up in the mostly fayalitic and dominated by iron oxides matrix of the T2b slag.

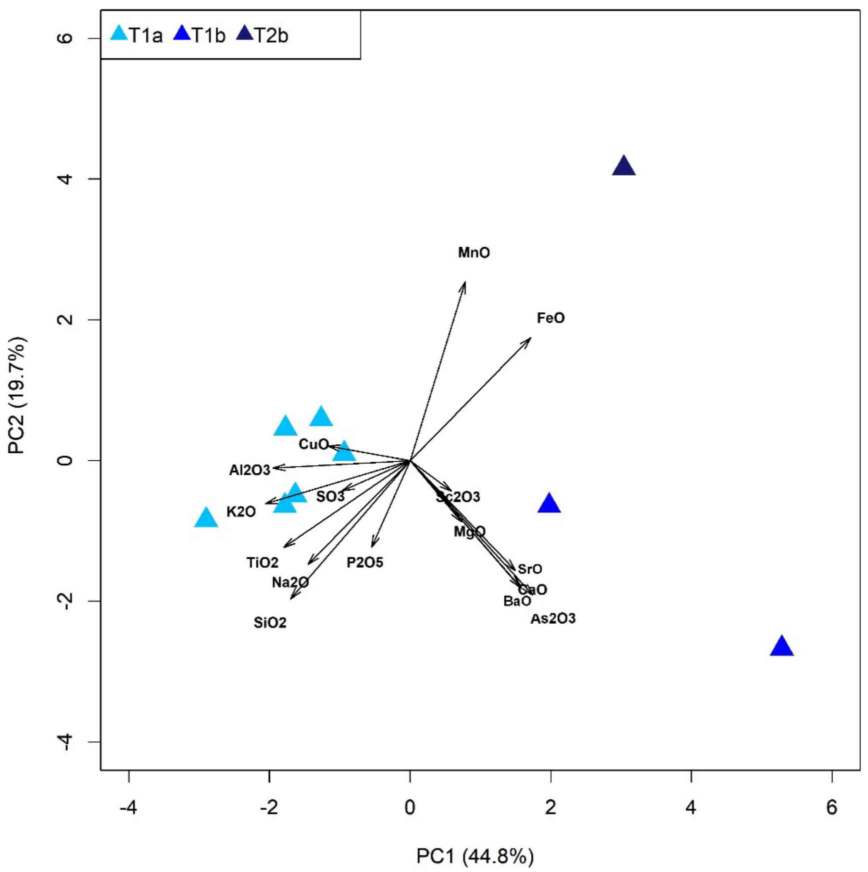

Fig. 13. PCA score plot of SEM-EDS bulk values of slag types T1a, T1b and T2b from Taldysai, previously normalised to 100%.

The ternary plot of all Taldysai bulk slag composition in the CaO-SiO_2-FeO equilibrium system highlights the different viscosity ranges at liquidus temperature observed between slags T1a, T1b and T2b (**Figure 14**). The upper region of the plot, silica-rich, is occupied by slags of the Cu production line (T1a). This reflects the high silica content obtained by fusing copper ores presenting a siliceous gangue (**Figure 9**). On the other hand, arsenical copper was smelted in a two-step process, very likely within crucibles in bowl-shaped above-ground furnaces, which explains the high lime content. Thus, the first step of Cu-As smelting (T1b) shifts towards the FeO corner, as sulfur is reduced and forms matte phases and iron is released by reducing arsenic-rich ores, e.g. arsenopyrite or tennantite. FeO ends up in newly formed mineral phases such as speiss, but also fayalitic olivine and spinels with magnetite composition. The presence of spinels points to 'local' oxidising environment within the reaction vessel. We hypothesise that this could have taken place in crucible vessels within bowl-shaped above-ground furnaces; samples of these are currently under investigation. The resulting matte undergoes a further step of reduction to remove the remaining iron in the charge (T2b). This step reaches the most reducing conditions: wüstite forms while the arsenic content in prills lowers down due to partial volatilisation (Lechtman and Klein, 1999), but still produces a 'high arsenic' alloy (**Table 5**).

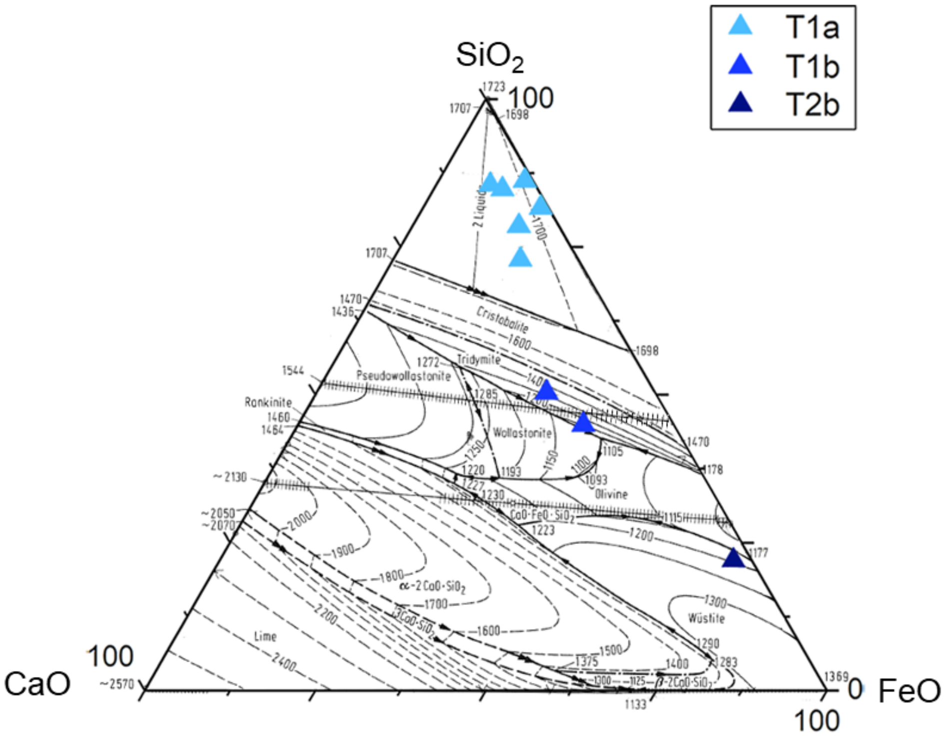

Fig. 14. Slag types from Taldysai T1a, T1b and T2b plotted in the ternary SiO_2-FeO-CaO equilibrium system. (Modified from Slag Atlas, 1995: 126, Figure 3.223).

Speaking of the ore charge for T1a, it was very likely cuprous sandstone, represented as a mix of copper oxides/carbonates and secondary sulfides like chalcocite and bornite, with varying concentrations of iron oxide and silica as gangue. These ores were therefore self-fluxing.

Noteworthy is that experimental smelting of cuprous sandstone from the Cis-Urals showed that very little to no fluxing was required (Rovira, 1999). Analyses of slags from the Bronze Age settlements of this area known to have likely exploited copper sandstone deposits would fit the same scenario (Ankushev et al., 2021: 21-22). In terms of the origins of such deposits for Taldysai, smelters were very likely using Dzhezkazgan ores. This is further supported by analyses of fragments of green minerals found at the settlement currently under investigation for the doctoral project of the first author and previously analysed minerals by Ankushev et al. (2020).

When it comes to arsenical copper production line (T1b and T2b), similarly to the smelting of chalcopyrite, it is possible to obtain arsenical copper by co-smelting copper oxides with copper or iron sulfarsenides (e.g. tennantite and arsenopyrite; Merkel and Shimada, 1988; Lechtman, 1991; Lechtman and Klein, 1999), which would result in the unintentional formation of speiss inclusions in slags (Hauptmann, 2020: 282). Another possibility includes the smelting of speiss from arsenopyrite to be then alloyed to copper as proposed by Rehren et al. (2012), although for the moment this option requires investigation of additional slag samples.

4.5 Taldysai and the 2nd millennium BC Eurasian Bronze Age metal production technology

The data collected on slag types T1a, T1b and T2b from Taldysai were further compared against a database of copper smelting debris from different production centres, in order to explore the 2nd millennium BC metalmaking technology in Eurasia and investigate any variance and/or similarities across this space and time (**Figure 8** and **Table 2**).

The metal production contexts we selected for comparative analyses, detailed in **Table 2**, bring together Bronze Age workshops in the proximity of ore fields in Italy, Cyprus, Austria, Georgia, Russian Federation and China. Compositional data collected on smelting slags from these sites were analysed with PCA in order to assess the main directions of variance in their chemistry.

The PCA score plot (**Figure 15**) highlights that the greatest variance derives from ore and fuel ash contamination (PC1), which generates specific sub-clusters for every slag group. On the other hand, PC2 defines a macro division between materials more impacted by FeO contents and those more dominated by silica-alumina-low titania.

Taldysai slags T1a fall alongside the highest loadings of silicon, aluminium, potash and titanium oxides considered the high silica gangue in copper sandstone. Taldysai slags T1b are also plotted in the area with more dominant silica, but also more magnesia, lime and arsenic, similar to those from Laoniupo (which has significantly higher arsenic signature). In our view, this may be linked to their formation in a different reaction vessel (such as a crucible), or to somewhat different quality of ores compared to those used for T1a production line. The high FeO scores include the T2b slag and the majority of the matte smelting slags from a chalcopyrite charge and almost completely depleted in metal from the Alps, Kamennyi-Ambar and Politiko Phorades. Among slags characterised by high FeO, it is possible to outline two plot areas defined by the angle between FeO-MnO and that between FeO-ZnO-BaO-SO_3 (this specific of the Caucasus), which are consistent with areas (e.g. the Alps and Western Georgia) with a distinct ore signal. Looking at the values and slags that plot away from the FeO predominance, the scores of slags shift in the direction of the fuel ash vectors (Na_2O, P_2O_5, MgO, CaO, K_2O) without a clear distinction between geographic areas (e.g. Taijiasi and other scores from the Caucasus area) as noted in the lower part of the **Figure 15**.

Interestingly, the sites of Taldysai (T2b), the Italian and Austrian Alps, Kamennyi-Ambar, Politiko Phorades and the Caucasus presented slags of similar quality despite having differences in the design of smelting installations/furnaces. For instance, the slag T2b (BAE 29) from Taldysai and flat slags from the Alps align alongside the FeO vector while the T2b slag from Taldysai was presumably produced in crucible within bowl-shaped furnaces, whereas sites in the Alps used shaft furnaces in which slags were likely left to cool down in. This example shows that the similar smelting output/slags can be produced from different types of smelting installations, however, it is the types of ores (here chalcopyrite or, in the case of Taldysai, an iron-arsenic rich ore) that produce comparable compositional results.

We suggest that different designs of furnace installations had implications in the efficiency of the extractive process, hence showing that similar smelting output could be achieved because of similar material properties of the smelting charge, namely ores, combustible and use of flux, combined differently. This is the case in point of archaeological slags of the T1a type we discussed in this paper, experimentally reproduced by I. Rusanov in a vaulted pit furnace such as those in Taldysai (Yermolayeva and Rusanov, 2022) and experimental copper slags obtained by Rovira (1999) in a crucible smelting. In these two trials, a similar type of copper ore was used (above).

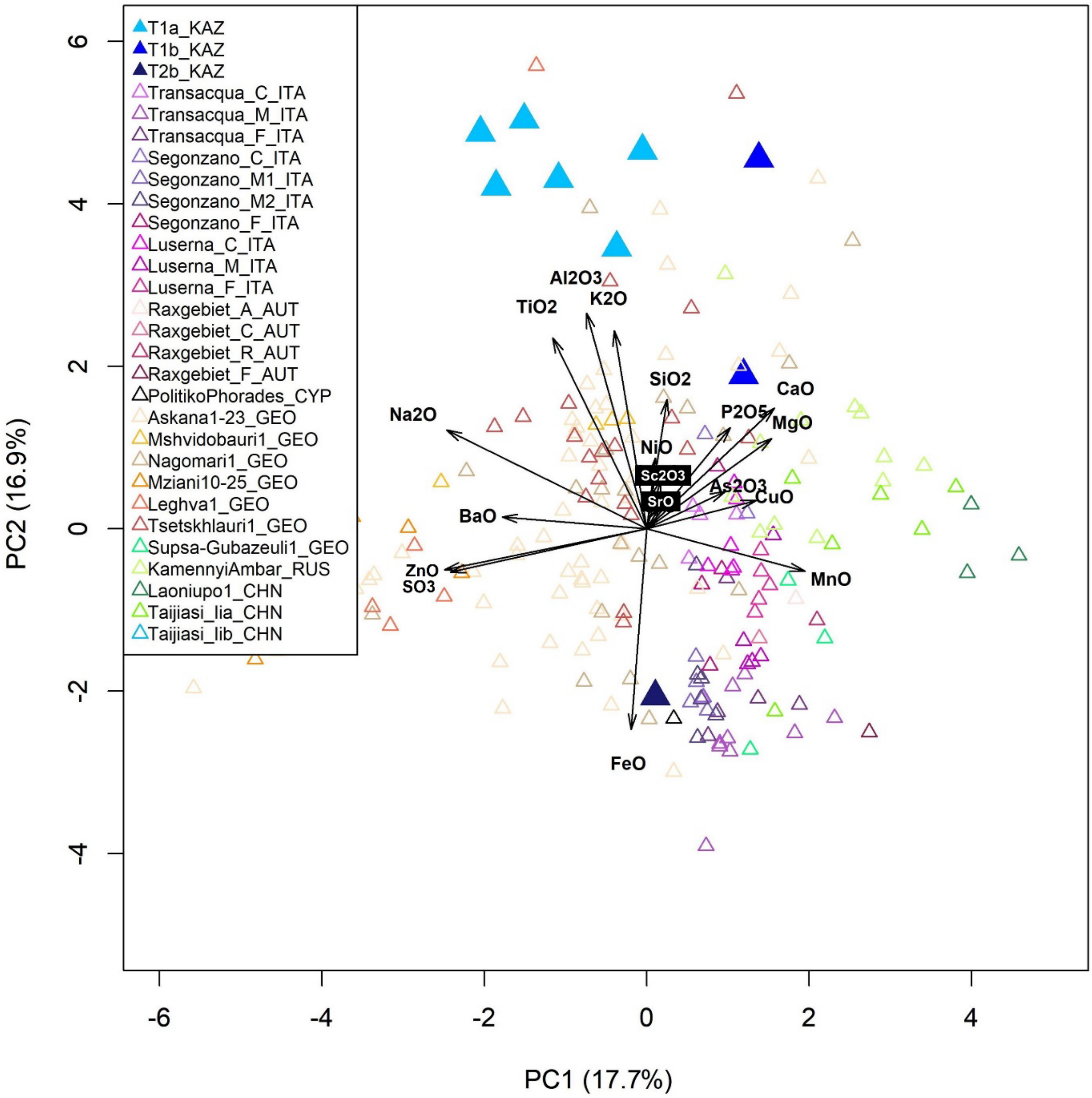

Fig. 15. PCA score plot of copper smelting slags bulk values of Taldysai (group T1a, T1b and T2b, bigger triangles) with respect to 2nd millennium BC metal production comparative sites detailed in Table 2. All values (wt%) previously normalised to 100%. Abbreviations as in original publications: A=amorphous; C=coarse; M=massive; F=flat; R=rich. Data are reported in Supplementary Material. Corresponding countries of sites are: KAZ (Kazakhstan), ITA (Italy), AUT (Austria), CYP (Cyprus), GEO (Georgia), RUS (Russian Federation), CHN (China).

5. Discussion

5.1 Smelting technology at Taldysai: a case of regional scale inventiveness

Our analysis showed evidence of two lines of metal production at the settlement of Taldysai. One was aiming to produce pure copper metal through co-smelting of copper oxides/carbonates with secondary sulfides such as chalcocite and bornite, resembling the cuprous sandstone available locally from Dzhezkazgan ores. The other exhibited the production of arsenical copper by exploiting arsenic and iron-rich minerals that were co-smelted with copper oxides and/or copper secondary sulfides, the latter presumably being of similar origin as those use for pure copper production. We propose tennantite or arsenopyrite as good candidates for the arsenic source; these also form part of the present-day mineralisation of Dzhezkazgan, although their exploitation during the Bronze Age is currently unknown. Based on our data the two metal production lines followed different protocols and were carried out in different furnace installations.

Copper extraction (T1a slags) was performed through a joint reaction within the vaulted pit furnaces with horizontal channel by co-smelting a charge of copper oxides and Cu/Cu-Fe sulfides (chalcocite and bornite). These mineral horizons were most likely geologically available in association. In support of this, experimental smelting conducted by I. Rusanov between 2012 and 2013 in a replica of the vaulted pit furnaces of Taldysai successfully produced copper metal from a charge of chalcocite ores from the Dzhezkazgan area (Artyuhova et al., 2013: 364-365; Yermolayeva and Rusanov, 2022). Smelting debris produced during these experimental trials resulted in slags that compared well to archaeological slags T1a (Calgaro and Radivojević, 2022). We also propose that primary sulfides (e.g. chalcopyrite) were not part of the charge and their rare presence in Taldysai slags may have been related to the heterogeneous nature of ore strata of the Dzhezkazgan deposit. This is supported by the scarce presence of chalcopyrite and low iron content in T1a slags. Artemyev and Ankushev (2019) and Ankushev et al. (2020) recently suggested the Dzhezkazgan cuprous sandstone ore deposit as the main source for copper ores at Taldysai, which has also been proposed for other metalmaking workshops identified in the Ulytau steppes and in the Bronze Age mines of Dzhezkazgan (Kuznetsova and Teplovodskaya, 1994; Margulan, 2020). Dzhezkazgan has long been identified as one the six centres for copper extraction exploited during the Bronze Age in Central Kazakhstan, alongside Kokshetau, Bayanaul, Uspenka-Karkaraly, the North Betpakdala and Balkash metallurgical centres (Berdenov, 2008; Yermolayeva, 2020). This is in addition to the Late Bronze Age mining centre in Kargaly in Southern Urals, where the exploitation of sandstone sources for copper metal has already been well documented (Chernykh, 2004). The use of copper ores mineralised in sandstone seems especially plausible considered the high amount of silica and quartz grains in T1a slags. Noteworthy, iron oxides and hydroxides are known to occur alongside copper ores here (above, Section 2), hence suggesting that the said ore charge might have been self-fluxing. Upon separation from the matte, copper metal would aggregate in droplets and sink at the bottom of the pit-furnace, from where it was recovered. T1a slags were also presumably mechanically crushed to collect any leftover metal.

With respect to arsenical copper, the production and consumption of copper-arsenic alloys in the Near East, Central Asia and Europe is documented since the early 4th millennium BC until well into the Late Bronze Age (Chernykh, 1966; Chernykh, 1992; Lechtman, 1999 and literature therein; Thornton et al., 2009).

In our case, arsenical copper was produced by co-smelting copper and/or iron sulfarsenide (e.g. tennantite, arsenopyrite, scorodite) with copper oxides or Cu secondary sulfides (above and Lechtman, 1996). The formation of speiss was more likely unintentional, as it can occur in the smelting systems that include copper, iron, sulfur and oxygen (Rehren et al., 2012). As in Sections 4.2 and 4.3, it is worth pointing out that in our case we recorded Cu-As metal prills in all slags related to arsenical copper, which is different from cases discussed by Thornton et al. (2009) and Rehren et al. (2012). Co-smelting of copper oxides and/or secondary sulfides with arsenopyrite or tennantite was most likely carried out in crucibles within bowl-shaped above-ground furnaces of Taldysai, as we noted that clay or fuel highly contributed to the formation of the slags of type T1b, compared to T1a slags.

The next step would be to further reduce and separate iron from the arsenical copper alloy. In our interpretation, this is represented with slag T2b (BAE 29), even though we acknowledge that at present this sample constitutes a single evidence. Nevertheless, the wüstite noticed in this sample points to more reducing atmosphere than for the other slags. No sulfur readings in metallic inclusions, nor matte phases were noticed in the slag microstructure, which would have formed out of the same ore charge noticed in group T1b.

Three types of Taldysai slags presented here correspond to two parallel lines of metal production presumably carried out since the earliest occupational phase of Taldysai, since one sample of group T1a and the arsenical copper-bearing slags (T1b and T2b) were collected in the Petrovka layers (c. 1900 - 1800 BC) of the northern complex. Evidence of arsenical copper production at the site is consistent with analyses of slags performed by Ankushev et al. (2020), who also noted slag materials related to tin bronze production. There is also a group of copper, arsenical copper, tin bronze and polymetallic alloys (arsenic-tin bronzes) metal artefacts and casting products analysed by Park (2020). This would mean that the ores used at the site of Taldysai included a range of copper, arsenic and tin-enriched mineralisations, which raises new questions concerning the supply routes of raw materials. The smelting of arsenical copper is documented for the Middle Bronze Age Sintashta-Petrovka layers (2000-1700 BC) in the Urals settlements, where arsenic occurs in mineralisation alongside copper oxides in form of copper arsenate (Ankushev et al. 2021). On the other hand, the presence of tin bronze artefacts at Taldysai brings into view the hypothesis of connections with the area of the Altai and northern or eastern Kazakhstan (Stöllner et al., 2013a; 2013b), or the use of closer sources such as the cassiterite deposit in the Souktal granite-gneiss massif, which is located in the Ulytau district (about 165 km to the north of Taldysai) (Satpaev, 1956); however, no data at present show ancient mining activities at this location.

5.2 Smelting technology in Eurasia: the broader perspective

From a broader perspective, at least one of the two steps of Bronze Age copper smelting (matting and matte smelting) can be spotted in each of the sites we selected for comparative analysis with Taldysai. The material evidence from these metalmaking centres allowed in some cases to follow the whole smelting process, such as in the Alps and in South-Western Caucasus, whereas others presented only a snapshot of one of the stages, i.e. Cyprus, the Southern Urals, the Chinese sites considered here.

Our results showed that technology of metal production had been mastered by metalsmiths for a wide range of sulfidic-based ore sources, which were processed differently in different geographic contexts to produce copper-based alloys, including arsenic and tin, depending on specific and desired material properties. In this sense, this comparative analysis of production debris highlighted a very heterogeneous picture characterised by variations from local to regional scale. Such variations are dictated by the interplay of several factors, such as the exploitation of ore sources with different signature, different recipes for (self)fluxing and fuel ratios, the ability in controlling redox atmosphere and the design of smelting installations/furnaces, which all together result in different solutions to extract copper metal.

Looking at different regional furnace designs, the vaulted pit furnace with horizontal channel model from Taldysai represents an evolutionary development from the furnaces documented in Middle Bronze Age Sintashta sites in the Urals up to the Zarafshan valley (Koryakova and Epimakhov, 2007; Grigoriev, 2015: 99; Avanesova, pers.comm.). Hence in this broader region of Southern Urals - Central Kazakhstan, such furnaces would be a regional choice to smelt copper metal.

A closer look at some of the smelting contexts from the Eastern Alps highlights another regional perspective: mineral ores were first roasted on platforms, and subsequent copper enrichment and matting would take place in shaft furnaces that could have been operated in tandem (Kraus et al., 2015: 301; Silvestri et al., 2015). These installations consisted of pit furnaces equipped with vertical shaft and built in stone slabs, like those arranged in battery at the Middle and Late Bronze Age Site 1 of the Eisenerzer Ramsau valley and Acqua Fredda (North-Eastern and Southern Alps). The contexts from the Caucasus considered here seemed to generally adapt to a similar production strategy from the Alps, including possible intermediate roasting(s) in open platforms, but conducting the multi-step matting in pit furnaces and final matte smelting in crucibles (Erb-Satullo et al., 2015: 269).

At the same time, smelting slags from Laoniupo analysed by Chen et al. (2017), which were considered to represent the matting step of production, appear strikingly similar to T1b slags from Taldysai for mineral phases and arsenic content in metallic prills (up to 32.4 wt%). In our opinion, this supports the hypothesis that the T2b slag from Taldysai would represent a further refining step of the matte produced by co-smelting arsenic-iron rich ores with copper oxides or secondary sulfides reflected in T1b slags.

The T2b slag from Taldysai aligns well for iron-silica ratio with all the slags of the last stage of copper metal production from Southern and North-Eastern Alps, Cyprus and the Southern Urals. A closer look to the diameter of metallic prills in all mentioned slags allows one to separate out metallurgical operations where copper metal separation was more efficient, or less successful. The exterior morphology of slags indicates that their efficient separation from the charge could be obtained by liquid buoyancy in pit furnace and slag formation as a thin top layer (in the Alps) or by skimming the slag surface of crucibles like in the Caucasus. All these protocols, generally paired by the same level of slag fluidity, reflect in in mineral phases habitus of slags observed.

High level technological knowledge and the repetitive scheme of typological designs across specific geographic areas require to be analysed within a wider perspective, taking into account considerations on production organisation and logistics. Network of ideas, not only raw materials like ores, or ingots/objects, were likely in place on local to regional scale, as suggested by the regional diffusion of smelting installations types and metal production recipes (also, Radivojević et al., 2019 and literature therein).

6. Conclusions

This study provided a glimpse into the metal production carried out at the Mid/Late Bronze Age workshop of Taldysai in Central Kazakhstan and preliminary information on the technological skill that fit well in the wider 2nd millennium BC metalmaking picture. Chemical analysis of a pilot sample of nine smelting slags allowed to distinguish two lines of metal production, copper and arsenical copper. These production lines were likely carried out in different smelting structures on the site.

Our comparative analysis with production debris from nine broadly contemporary metalmaking centres from the Alps to Central China, based on multivariate statistics of compositional data, highlighted a very heterogeneous picture resulting from several factors, such as the exploitation of ore sources with different signatures, different recipes for flux and fuel ratios, the ability to control the redox atmosphere and the design of furnaces, which altogether exhibit multiple pathways to achieve full or partial efficiency in copper extraction across the continent.

Our future work will involve collection of additional data on metallurgical debris from all different excavation complexes at Taldysai in order to expand the results collected thus far, and to understand how did this site fit in the network of metal knowledge, ores and products exchange in the Eurasian Steppe on a more fine-grained level.

Acknowledgements

This manuscript is based on IC's MSc thesis and continuing as her Doctoral research at the UCL Institute of Archaeology. IC acknowledges the Institute for Archaeo-Metallurgical Studies (IAMS) for funding her MSc studies at the Institute of Archaeology of UCL and part of her PhD through the Tylecote Fund. The London Arts and Humanities Partnership (LAHP - AHRC) is further thanked for funding IC's Doctoral studies at the UCL Institute of Archaeology. MR is indebted to the funding received from the McDonald Institute for Archaeological Research, University of Cambridge, between 2015 and 2017, which allowed her to start the Bronze Age metallurgy research in Kazakhstan and specifically at the site of Taldysai in this case. All authors remain indebted to the leadership of the A.Kh. Margulan Institute of Archaeology in Almaty for facilitating and supporting this international collaboration.

Declarations of interest

The authors declare no competing interests.

Authors' contribution

IC prepared part of the slag samples (slags T1b) and carried out their SEM-EDS analysis, performed treatment and interpretation of all optical, chemical and compositional legacy data presented here, carried out this study and wrote this manuscript. MR selected the slags samples from Taldysai discussed here, supervised this study and co-wrote the manuscript. UV prepared the rest of slag samples (slags T1a and T2b) discussed in this paper and collected related SEM-EDS raw data. ASY excavated and provided access to the Taldysai material collection and field documentation for analysis.

Appendix

Table A1.
Calculations to determine the accuracy of CRM BHVO-2 used for analysis. Some elements are not reported either because not certified for the CRM or because in concentration below detection limit. Bulk analyses of samples BAE 29-45 are scaled on BHVO-2 by, e.g., $M_{BAE30\ average}$ - E%*$M_{BAE30\ average}$/100. Data normalised to 100% and expressed as wt%. M_{CRM} = Measured CRM; C_{CRM} = Certified CRM. SD = Standard Deviation. Bdl = Beyond Detection Limit.

Sample	Measures	Na_2O	MgO	Al_2O_3	SiO_2	P_2O_5	SO_3	K_2O	CaO	Sc_2O_3	TiO_2	MnO	FeO	CoO	NiO	CuO	As2O3	SrO	BaO
Measured CRM BHVO-2 average	7	2.3	7.2	13.7	49.8	0.2	bdl	0.5	11.6	bdl	2.9	bdl	11.6	bdl	bdl	bdl	bdl	bdl	bdl
SD		0.1	0.1	0.1	0.7	0.2	-	0.0	0.1	-	0.1	-	0.9	-	-	-	-	-	-
Certified CRM BHVO-2		2.2	7.2	13.5	49.9	0.3	bdl	0.5	11.4	bdl	2.7	bdl	12.3	bdl	bdl	bdl	bdl	bdl	bdl
Error (M_{CRM}-C_{CRM})		**0.0**	**0.0**	**0.2**	**-0.1**	**-0.1**	**-**	**0.0**	**0.2**	**-**	**0.2**	**-**	**-0.7**	**-**	**-**	**-**	**-**	**-**	**-**
%Error (M_{CRM}/C_{CRM}*100)		**1.4**	**0.2**	**1.5**	**-0.2**	**-28.0**	**-**	**3.2**	**1.5**	**-**	**6.3**	**-**	**-6.0**	**-**	**-**	**-**	**-**	**-**	**-**
Group T1a																			
BAE 30 average	3	1.9	0.8	25.5	47.7	-	-	4.1	0.5	-	0.7	-	8.8	-	-	-	-	-	-
BAE 31 average	3	2.5	1.0	17.6	49.4	2.3	-	2.3	5.7	-	0.6	-	13.4	-	-	-	-	-	-
BAE 32 average	3	1.8	0.5	15.9	43.5	0.7	-	2.5	3.3	-	0.4	-	4.3	-	-	-	-	-	-
BAE 33 average	3	2.8	1.1	19.3	53.7	1.2	-	2.8	4.0	-	0.6	-	11.3	-	-	-	-	-	-
BAE 34 average	3	3.1	0.2	17.2	56.9	1.5	-	3.6	0.8	-	0.5	-	8.8	-	-	-	-	-	-
BAE 35 average	4	2.8	0.7	15.6	55.7	1.3	-	2.7	3.3	-	0.4	-	7.0	-	-	-	-	-	-

Group T1b																			
BAE 40 average	3	2.0	3.9	9.1	40.2	1.3	-	2.0	12.5	-	0.5	-	28.5	-	-	-	-	-	-
BAE 45 average	2	2.1	1.1	6.3	37.5	0.8	-	0.8	10.9	-	0.2	-	36.9	-	-	-	-	-	-
Group T2b																			
BAE 29 average	2	1.6	0.4	8.0	19.3	-	-	0.5	1.5	-	1.5	-	70.2	-	-	-	-	-	-

Table A2.

SEM-EDS compositional values of metallic prills detected in slag groups T1a, T1b and T2b from Taldysai. Data normalised to 100% and expressed as at%. SD = Standard Deviation. Bdl = Beyond Detection Limit.

Sample	Measures		O	S	Fe	Co	Ni	Cu	As	Ag
Group T1a										
BAE 30	8	Min	1.2	bdl	0.0	bdl	bdl	95.1	bdl	bdl
		Average	**1.7**	**-**	**0.5**	**-**	**-**	**97.8**	**-**	**-**
		Max	2.2	bdl	3.4	bdl	bdl	98.4	bdl	bdl
		SD	0.3	-	1.2	-	-	1.1	-	-
BAE 31	4	Min	1.5	0.0	0.0	bdl	bdl	95.4	bdl	bdl
		Average	**2.0**	**1.7**	**0.1**	**-**	**-**	**96.2**	**-**	**-**
		Max	2.3	2.4	0.3	bdl	bdl	97.3	bdl	bdl
		SD	0.4	1.1	0.2	-	-	0.8	-	-
BAE 32	1		bdl	2.9	bdl	bdl	bdl	97.1	bdl	bdl
BAE 33	3	Min	1.6	0.0	0.0	bdl	bdl	95.0	bdl	bdl
		Average	**2.1**	**1.4**	**0.2**	**-**	**-**	**96.2**	**-**	**-**
		Max	2.4	2.2	0.5	bdl	bdl	98.4	bdl	bdl
		SD	0.4	1.2	0.2	-	-	1.9	-	-
BAE 34	3	Min	1.9	0.0	0.0	bdl	bdl	92.8	bdl	bdl
		Average	**2.4**	**2.3**	**0.6**	**-**	**-**	**94.8**	**-**	**-**
		Max	2.7	4.7	1.1	bdl	bdl	96.4	bdl	bdl
		SD	0.4	2.3	0.5	-	-	1.8	-	-
BAE 35	5	Min	0.0	0.0	0.0	bdl	bdl	95.4	bdl	bdl
		Average	**2.4**	**0.4**	**0.3**	**-**	**-**	**96.9**	**-**	**-**
		Max	3.9	1.5	0.9	bdl	bdl	99.1	bdl	bdl
		SD	1.5	0.7	0.4	-	-	1.4	-	-
Group T1b										
BAE 40 Arsenic-poor phase	12	Min	1.7	bdl	bdl	bdl	bdl	84.5	0.4	bdl
		Average	**2.4**	**0.0**	**2.5**	**0.0**	**-**	**89.9**	**5.4**	**0.0**
		Max	4.8	0.0	4.2	0.0	bdl	91.6	8.6	0.0
		SD	1.0	0.0	1.5	0.0	-	2.9	2.4	0.0
BAE 40 Arsenic-rich phase	2	Min	1.8	bdl	0.7	bdl	bdl	70.3	25.7	bdl
		Average	**1.8**	**0.0**	**1.5**	**-**	**-**	**71.0**	**25.8**	**-**
		Max	1.8	0.0	2.3	bdl	bdl	71.7	25.9	bdl
		SD	0.0	-	1.1	-	-	1.0	0.1	-
BAE 45 Arsenic-poor phase	3	Min	1.6	bdl	bdl	bdl	bdl	94.2	2.4	bdl
		Average	**1.8**	**-**	**0.2**	**-**	**-**	**95.3**	**2.8**	**-**
		Max	1.9	bdl	0.1	bdl	bdl	95.9	3.7	bdl
		SD	0.2	-	0.1	-	-	0.9	0.8	-
BAE 45 Arsenic-rich phase	9	Min	2.1	0.4	0.2	bdl	bdl	65.9	16.1	bdl
		Average	**4.5**	**0.6**	**1.8**	**-**	**-**	**68.5**	**24.7**	**0.0**
		Max	16.8	1.5	1.5	bdl	bdl	71.4	27.9	0.0
		SD	4.8	0.4	1.5	-	-	2.5	3.4	0.0
Group T2b										
BAE 29	2	Min	1.8	bdl	2.2	bdl	0.4	88.0	6.5	bdl
		Average	2.1	**-**	**2.5**	**-**	**0.6**	**88.0**	**6.7**	**-**
		Max	**2.5**	bdl	2.7	bdl	0.9	88.1	7.0	bdl

		SD	0.5	-	0.4	-	0.4	0.1	0.4	-

Table A3.
SEM-EDS compositional values of sulfidic phases detected in slags groups T1a and T1b. Data normalised to 100% and expressed as wt%. SD = Standard Deviation. Bdl = Beyond Detection Limit.

Sample	Measures		O	S	Cr	Fe	Cu	As	Se	Zr	Ag	Bi
Group T1a												
BAE 30	4	Min	0.0	1.4	bdl	0.0	80.7	bdl	bdl	bdl	bdl	bdl
		Average	**2.6**	**14.7**	**-**	**0.3**	**82.4**	**-**	**-**	**-**	**-**	**-**
		Max	10.6	19.2	bdl	0.6	87.3	bdl	bdl	bdl	bdl	bdl
		SD	5.3	8.8	-	0.3	3.3	-	-	-	-	-
BAE 31	3	Min	0.0	19.0	bdl	bdl	80.5	bdl	bdl	bdl	bdl	bdl
		Average	**0.1**	**19.2**	-	bdl	**80.6**	-	-	-	-	-
		Max	0.4	19.5	bdl	bdl	80.7	bdl	bdl	bdl	bdl	bdl
		SD	0.3	0.3	-	-	0.1	-	-	-	-	-
BAE 32	1		**bdl**	**23.3**	**bdl**	**10.0**	**66.8**	**bdl**	**bdl**	**bdl**	**bdl**	**bdl**
BAE 33	3	Min	0.0	17.9	bdl	bdl	81.6	bdl	bdl	bdl	bdl	bdl
		Average	**0.2**	**18.1**	**-**	**-**	**81.8**	**-**	**-**	**-**	**-**	**-**
		Max	0.5	18.2	bdl	bdl	82.0	bdl	bdl	bdl	bdl	bdl
		SD	0.3	0.2	-	-	0.2	-	-	-	-	-
BAE 34	4	Min	0.0	14.8	bdl	0.0	74.3	bdl	bdl	bdl	bdl	bdl
		Average	**0.8**	**19.5**	**-**	**2.3**	**77.4**	**-**	**-**	**-**	**-**	**-**
		Max	3.1	21.7	bdl	4.0	82.1	bdl	bdl	bdl	bdl	bdl
		SD	1.5	3.2	-	1.9	3.5	-	-	-	-	-
BAE 35	4	Min	0.0	17.0	bdl	0.0	53.2	bdl	bdl	bdl	0.0	bdl
		Average	**0.3**	**21.5**	**-**	**6.2**	**71.9**	**-**	**-**	**-**	**0.2**	**-**
		Max	1.0	28.7	bdl	17.5	82.0	bdl	bdl	bdl	0.6	bdl
		SD	0.5	5.1	-	7.9	12.9	-	-	-	0.3	-
Group T1b												
BAE 40	8	Min	0.7	11.7	bdl	1.5	68.1	0.4	0.7	bdl	bdl	bdl
		Average	**1.4**	**16.5**	**0.0**	**2.5**	**72.3**	**5.7**	**1.2**	**0.0**	**0.0**	**0.4**
		Max	2.0	19.5	0.1	3.8	76.6	15.3	2.1	0.2	0.2	0.9
		SD	0.6	3.6	-	0.9	3.3	6.9	0.6	-	-	0.4

Table A4.
SEM-EDS compositional values of sulfidic phases detected in slags groups T1a and T1b. Data normalised to 100% and expressed as at%. SD = Standard Deviation. Bdl = Beyond Detection Limit.

Sample	Measures		O	S	Cr	Fe	Cu	As	Se	Zr	Ag	Bi
Group T1a												
BAE 30	4	Min	0.0	23.5	bdl	0.0	50.2	bdl	bdl	bdl	bdl	bdl
		Average	**6.5**	**29.8**	**-**	**0.1**	**63.6**	**-**	**-**	**-**	**-**	**-**
		Max	26.1	32.0	bdl	0.2	68.1	bdl	bdl	bdl	bdl	bdl
		SD	13.1	4.2	-	0.1	8.9	-	-	-	-	-
BAE 31	3	Min	0.0	31.3	bdl	bdl	67.2	bdl	bdl	bdl	bdl	bdl
		Average	**0.5**	**31.9**	**-**	**-**	**67.6**	**-**	**-**	**-**	**-**	**-**
		Max	1.5	32.4	bdl	bdl	67.9	bdl	bdl	bdl	bdl	bdl
		SD	0.8	0.5	-	-	0.3	-	-	-	-	-
BAE 32	1		bdl	37.1	bdl	9.1	53.8	bdl	bdl	bdl	bdl	bdl
BAE 33	3	Min	0.0	29.7	bdl	bdl	68.5	bdl	bdl	bdl	bdl	bdl
		Average	**0.6**	**30.2**	**-**	**-**	**69.2**	**-**	**-**	**-**	**-**	**-**
		Max	1.8	30.7	bdl	bdl	69.7	bdl	bdl	bdl	bdl	bdl
		SD	1.0	0.5	-	-	0.6	-	-	-	-	-
BAE 34	4	Min	bdl	23.7	bdl	0.0	61.0	bdl	bdl	bdl	bdl	bdl

		Average	**-**	**31.8**	**-**	**2.2**	**63.6**	**-**	**-**	**-**	**-**	**-**
		Max	9.9	35.2	bdl	3.8	66.4	bdl	bdl	bdl	bdl	bdl
		SD	-	5.4	-	1.8	2.5	-	-	-	-	-
BAE 35	4	Min	0.0	28.1	bdl	0.0	40.9	bdl	bdl	bdl	0.0	bdl
		Average	**0.9**	**34.5**	**-**	**5.5**	**59.1**	**-**	**-**	**-**	**0.1**	**-**
		Max	3.4	43.6	bdl	15.3	68.5	bdl	bdl	bdl	0.3	bdl
		SD	1.7	6.6	-	6.8	12.6	-	-	-	0.1	-
Group T1b												
BAE 40	8	Min	2.4	19.9	bdl	1.6	58.5	0.3	0.5	bdl	bdl	bdl
		Average	**4.8**	**27.3**	**0.1**	**2.4**	**60.6**	**4.1**	**0.8**	**0.1**	**0.1**	**0.1**
		Max	7.1	31.8	0.1	3.5	63.2	11.3	1.4	0.1	0.1	0.2
		SD	2.0	5.4	0.0	0.8	1.7	5.1	0.4	0.0	0.0	0.1

Table A5.
SEM-EDS compositional values of Fe-Cu-As metallic inclusions ('speiss') in sample BAE 45. Data normalised to 100% and expressed as wt%. SD = Standard Deviation. Bdl = Beyond Detection Limit.

Sample	Measures	O	S	Fe	Co	Ni	Cu	As	Se	Sr
BAE 45	1	0.0	0.1	20.5	0.5	0.1	39.1	39.5	0.3	0.1
	2	2.5	0.4	6.5	0.1	0.0	63.1	27.4	0.0	0.0

Table A6.
SEM-EDS compositional values of Fe-Cu-As metallic inclusions ('speiss') in sample BAE 45. Data normalised to 100% and expressed as at%. SD = Standard Deviation. Bdl = Beyond Detection Limit.

Sample	Measures	O	S	Fe	Co	Ni	Cu	As	Se	Sr
BAE 45	1	54.1	0.1	11.4	0.2	0.1	19.0	15.0	0.1	0.0
	2	53.1	0.3	3.8	0.1	0.0	32.1	10.7	0.0	bdl

Table A7 SEM-EDS compositional values of pyroxene phases detected in slags group T1b. Data normalised to 100% and expressed as wt%. SD = Standard Deviation. Bdl = Beyond Detection Limit.

Sample	Phase	Measures		Na_2O	MgO	Al_2O_3	SiO_2	P_2O_5	SO_3	K_2O	CaO	Sc_2O_3	TiO_2	V_2O_5	Cr_2O_3	MnO	FeO	CoO	NiO	CuO	SeO_2	SrO	Sb_2O_5	BaO
BAE 40	Augite	27	Min	0.2	4.4	6.5	41.0	0.6	bdl	bdl	16.0	bdl	0.4	bdl	bdl	bdl	16.0	bdl	0.0	bdl	bdl	bdl	bdl	bdl
			Average	**0.6**	**6.4**	**8.0**	**42.8**	**0.9**	**0.0**	**0.6**	**19.7**	**0.1**	**0.6**	**0.0**	**0.0**	**0.1**	**19.9**	**0.0**	**0.0**	**0.1**	**-**	**0.2**	**-**	**0.0**
			Max	1.9	7.7	9.1	44.3	1.2	0.1	2.8	22.0	0.2	0.7	0.2	0.1	0.2	23.5	0.2	0.1	1.3	bdl	0.6	bdl	0.3
			SD	0.4	1.0	0.7	1.0	0.2	0.0	0.7	1.7	0.1	0.1	0.0	0.0	0.1	1.9	0.0	0.0	0.3	-	0.2	-	0.1
BAE 45	Hedenbergite	10	Min	0.3	0.7	3.9	40.9	0.5	bdl	bdl	12.1	bdl	0.0	bdl	bdl	0.0	23.9	bdl	bdl	bdl	bdl	bdl	bdl	bdl
			Average	**0.6**	**3.0**	**4.9**	**43.6**	**0.7**	**0.0**	**0.2**	**20.2**	**0.1**	**0.2**	-	-	**0.0**	**25.9**	**0.1**	-	**0.1**	**0.0**	**0.3**	**0.0**	**0.0**
			Max	2.3	4.1	7.0	44.9	0.9	0.0	1.8	22.2	0.2	0.3	bdl	bdl	0.1	33.4	0.2	bdl	0.5	0.0	0.6	0.2	0.2
			SD	0.6	1.0	0.8	1.1	0.2	0.0	0.6	2.9	0.1	0.1	-	-	0.0	2.9	0.1	-	0.1	-	0.2	-	-

Table A8. SEM-EDS compositional values of pyroxene phases detected slags group T1b. Data normalised to 100% and expressed as at%. SD = Standard Deviation. Bdl = Beyond Detection Limit.

Sample	Phase	Measures		O	Na	Mg	Al	Si	P	S	K	CaO	Sc	Ti	V	Cr	Mn	Fe	Co	Ni	Cu	Se	Sr	Sb	Ag	Ba
BAE 40	Augite	27	Min	59.1	0.2	2.6	3.0	16.4	0.2	bdl	bdl	6.8	bdl	0.1	bdl	bdl	bdl	5.2	bdl	bdl	bdl	bdl	bdl	bdl	bdl	bdl
			Average	**59.5**	**0.5**	**3.7**	**3.7**	**16.8**	**0.3**	**0.0**	**0.3**	**8.3**	**0.1**	**0.2**	**0.1**	**0.0**	**0.0**	**6.6**	**0.0**	**0.0**	**0.1**	**-**	**0.1**	**-**	**0.0**	**-**
			Max	59.7	1.5	4.5	4.3	17.5	0.4	0.0	1.4	9.2	0.1	0.2	0.1	-	0.1	7.9	0.1	0.1	0.1	bdl	0.2	bdl	0.0	0.1
			SD	0.1	0.3	0.6	0.3	0.3	0.1	0.0	0.3	0.7	0.0	0.0	-	0.0	0.0	0.0	0.0	0.0	0.1	-	0.0	-	0.0	-
BAE 45	Hedenbergite	10	Min	58.9	0.3	0.4	1.9	17.0	0.2	bdl	bdl	5.4	bdl	0.0	bdl	bdl	0.0	7.7	bdl	bdl	bdl	bdl	bdl	bdl	bdl	bdl
			Average	**59.5**	**0.5**	**1.8**	**2.4**	**17.7**	**0.2**	**0.0**	**0.1**	**8.8**	**0.0**	**0.1**	**-**	**-**	**0.0**	**8.8**	**0.0**	**-**	**0.0**	**0.0**	**0.1**	**0.0**	**-**	**0.0**
			Max	59.6	1.9	2.5	2.7	18.1	0.3	0.0	1.0	9.6	0.1	0.1	bdl	bdl	0.0	11.6	0.1	bdl	0.1	0.0	0.1	0.0	bdl	0.0
			SD	0.2	0.5	0.6	0.4	0.4	0.1	0.0	0.3	1.2	0.0	0.0	-	-	0.0	1.1	0.0	-	0.0	-	0.0	-	-	-

Table A9. SEM-EDS compositional values of fayalite phases detected in slags group T1b. Data normalised to 100% and expressed as wt%. SD = Standard Deviation. Bdl = Beyond Detection Limit.

Sample	Phase	Measures		Na_2O	MgO	Al_2O_3	SiO_2	P_2O_5	SO_3	K_2O	CaO	Sc_2O_3	TiO_2	MnO	FeO	CoO	CuO	As_2O_3	SrO
BAE 40	Fayalite	6	Min	0.0	8.1	0.3	32.2	0.3	bdl	0.1	2.7	bdl	0.1	0.2	40.5	0.2	bdl	bdl	bdl

			Average	**0.6**	**11.5**	**2.4**	**34.1**	**0.4**	-	**0.6**	**3.6**	-	**0.1**	**0.3**	**46.0**	**0.3**	-	-	-
			Max	1.4	13.6	4.1	35.9	0.7	bdl	1.0	4.5	bdl	0.2	0.3	52.2	0.3	bdl	bdl	bdl
			SD	0.6	1.9	1.6	1.4	0.2	-	0.4	0.7	-	0.0	0.0	4.3	0.0	-	-	-
BAE 45	Fayalite	4	Min	0.2	0.7	0.2	30.0	0.2	bdl	0.2	3.4	bdl	bdl	0.0	20.4	bdl	bdl	bdl	bdl
			Average	**1.0**	**3.4**	**3.5**	**40.0**	**0.5**	**0.0**	**0.7**	**10.9**	**0.1**	**0.1**	**0.1**	**39.4**	**0.2**	**0.1**	**0.1**	**0.1**
			Max	1.8	6.6	6.8	49.2	1.1	0.0	1.5	16.3	0.1	0.2	0.2	56.9	0.4	0.2	0.3	0.4
			SD	0.7	2.4	2.7	8.3	0.4	0.0	0.5	6.1	0.1	0.1	0.1	16.7	0.2	0.1	0.2	0.2

Table A10. SEM-EDS compositional values of fayalite phases detected in slags group T1b. Data normalised to 100% and expressed as at%. SD = Standard Deviation. Bdl = Beyond Detection Limit.

Sample	Phase	Measures		O	Na	Mg	Al	Si	P	S	K	Ca	Sc	Ti	Mn	Fe	Co	Cu	As	Sr
BAE 40	Fayalite	6	Min	57.2	0.0	5.2	0.2	14.2	0.1	bdl	0.1	0.3	bdl	0.0	0.0	14.1	0.1	bdl	bdl	bdl
			Average	**57.5**	**0.5**	**7.3**	**1.2**	**14.6**	**0.2**	-	**0.4**	**1.6**	-	**0.0**	**0.1**	**16.5**	**0.1**	-	-	-
			Max	57.8	1.2	8.6	1.9	14.9	0.2	bdl	0.5	2.1	bdl	0.1	0.1	19.2	0.1	bdl	bdl	bdl
			SD	0.2	0.5	1.2	0.8	0.3	0.1	-	0.2	0.3	-	0.0	0.0	1.9	0.0	-	-	-
BAE 45	Fayalite	4	Min	57.1	0.2	0.5	0.1	13.7	0.1	bdl	0.1	1.7	bdl	bdl	0.0	6.6	bdl	bdl	bdl	bdl
			Average	**58.7**	**0.8**	**2.2**	**1.7**	**16.7**	**0.2**	**0.0**	**0.4**	**4.7**	**0.0**	**0.0**	**0.0**	**14.4**	**0.1**	**0.0**	**0.0**	**0.0**
			Max	60.0	1.4	4.5	3.1	19.2	0.4	0.0	0.8	8.4	0.1	0.1	0.1	21.7	0.2	0.1	0.1	0.1
			SD	1.4	0.5	1.7	1.2	2.7	0.2	0.0	0.4	3.4	0.0	0.0	0.0	7.7	0.1	0.0	0.0	0.1

Table A11. SEM-EDS compositional values of spinel phases detected in slags group T1b. Data normalised to 100% and expressed as wt%. SD = Standard Deviation. Bdl = Beyond Detection Limit.

Sample	Phase	Measures		Na_2O	MgO	Al_2O_3	SiO_2	P_2O_5	SO_3	K_2O	CaO	Sc_2O_3	TiO_2	V_2O_5	Cr_2O_3	MnO	FeO	CoO	NiO	CuO	As2O3	SeO_2	SrO	Sb_2O_5
BAE 40	Spinel	21	Min	bdl	0.5	0.4	0.3	bdl	bdl	0.0	0.3	bdl	0.4	bdl	bdl	bdl	74.3	bdl	bdl	bdl	bdl	bdl	bdl	bdl
			Average	**0.3**	**1.5**	**3.3**	**4.0**	**0.1**	**0.0**	**0.4**	**1.0**	**0.0**	**0.8**	**0.0**	**0.1**	**0.1**	**87.6**	**0.4**	**0.0**	**0.3**	-	**0.0**	**0.0**	**0.0**
			Max	2.2	5.4	5.6	12.6	0.4	0.2	2.1	2.6	0.0	1.7	0.2	0.4	0.3	94.9	0.6	0.2	2.4	bdl	0.0	0.4	0.3
			SD	0.6	1.3	1.4	3.5	0.1	0.0	0.4	0.7	0.0	0.5	0.1	0.1	0.1	6.4	0.1	-	0.6	-	-	0.1	-
BAE 45	Spinel	7	Min	bdl	0.3	1.6	0.2	bdl	bdl	bdl	0.2	bdl	0.2	bdl	bdl	bdl	92.4	0.3	bdl	bdl	bdl	bdl	bdl	bdl
			Average	**0.0**	**0.5**	**2.7**	**0.5**	**0.0**	**0.0**	**0.0**	**0.4**	**0.0**	**0.6**	**0.1**	**0.1**	**0.0**	**94.4**	**0.4**	-	**0.2**	**0.0**	-	**0.0**	-
			Max	0.2	0.9	4.0	1.0	0.0	0.0	0.0	0.5	0.0	1.1	0.2	0.4	0.1	95.9	0.6	bdl	0.7	0.0	bdl	0.0	bdl
			SD	0.1	0.2	0.8	0.3	0.0	0.0	0.0	0.1	0.0	0.4	0.1	0.2	0.0	1.4	0.1	-	0.2	0.0	-	0.0	-

Table A12. SEM-EDS compositional values of spinel phases detected in slags group T1b. Data normalised to 100% and expressed as at%. SD = Standard Deviation. Bdl = Beyond Detection Limit.

Sample	Phase	Measures		O	Na	Mg	Al	Si	P	S	K	Ca	Sc	Ti	V	Cr	Mn	Fe	Co	Ni	Cu	As	Se	Sr	Sb
BAE 40	Spinel	21	Min	50.2	bdl	0.5	0.4	0.2	bdl	bdl	0.0	0.2	bdl	0.1	bdl	bdl	bdl	32.0	bdl	bdl	bdl	bdl	bdl	bdl	bdl
			Average	**51.7**	**0.5**	**1.3**	**2.1**	**2.1**	**0.0**	**0.0**	**0.3**	**0.6**	**0.0**	**0.3**	**0.1**	**0.1**	**0.1**	**40.8**	**0.2**	**0.1**	**0.3**	-	**0.0**	**0.1**	**0.1**
			Max	54.0	2.2	3.3	3.5	6.5	0.2	0.1	1.4	1.3	0.0	0.7	0.1	0.2	0.1	47.9	0.3	0.1	1.0	bdl	0.0	0.1	0.1
			SD	1.0	0.6	1.1	0.9	1.8	0.1	0.0	0.3	0.4	0.0	0.2	0.0	0.0	0.0	4.5	0.0	-	0.3	-	-	0.1	-
BAE 45	Spinel	7	Min	50.4	bdl	0.2	1.1	0.1	bdl	bdl	bdl	0.1	bdl	0.1	bdl	bdl	bdl	44.2	0.1	bdl	bdl	bdl	bdl	bdl	bdl
			Average	**50.8**	**0.0**	**0.4**	**1.9**	**0.3**	**0.0**	**0.0**	**0.0**	**0.2**	**0.0**	**0.3**	**0.0**	**0.0**	**0.0**	**45.7**	**0.2**	-	**0.1**	**0.0**	-	**0.0**	-
			Max	51.2	0.2	0.8	2.2	0.6	0.0	0.0	0.0	0.3	0.0	0.5	0.1	0.2	0.0	46.9	0.3	bdl	0.3	0.0	bdl	0.0	bdl
			SD	0.3	0.1	0.2	0.6	0.2	0.0	0.0	0.0	0.1	0.0	0.2	0.0	0.1	0.0	1.0	0.0	-	0.1	0.0	-	0.0	-

References

Addis, A., Angelini, I., Nimis, P., Artioli, G., 2016. Late Bronze Age copper smelting slags from Luserna (Trentino, Italy): interpretation of the metallurgical process. Archaeometry, 58, 1, 96-114. https://doi.org/10.1111/arcm.12160.

Addis, A., Angelini, I., Artioli, G., 2017. Late Bronze Age copper smelting in the southeastern Alps: how standardized was the smelting process? Evidence from Transacqua and Segonzano, Trentino, Italy. Archaeol. Anthrop. Sci., 9, 5. https://doi.org/10.1007/s12520-016-0462-5.

Allentoft, M.E., Sikora, M., Sjogren, K-G., Rasmussen, S., Rasmussen, M., Stenderup, J., Damgaard, P.B., Schroeder, H., Torbjorn, A., Ahlstrom, T., et al., 2015. Population genomics of Bronze Age Eurasia. Nature, 522, 167-172. https://doi.org/10.1038/nature14507.

Ankushev, M.N., Artemyev, D.A., Blinov, I.A., 2020. Chapter 2. Bronze Age metallurgy of the settlement Taldysai: ores, slags, alloying [Глава 2. Металлургия Бронзого Века на поселении Талдысай: руды, шлаки, легирование], in: Kurmankulov, Zh. (Ed.), Taldysai. Settlement of ancient metallurgists of the Late Bronze Age in the Ulytau Steppe. Collective Monograph [Талдысай - Поселение древних металлургов Позднегобронзого Века в Улитаиской степи. Коллективная монография]. Almaty: Institute of Archaeology named after A.Kh. Margulan, pp. 72-93 (in Russian).

Ankushev, M.N., Artemyev, D.A., Blinov, I.A., Bogdanov, S.V., 2021. Bronze Age metallurgical slags from the South Urals: types, mineralogy and copper sources. Period. Mineral., 90, 5-25. https://doi.org/10.13133/2239-1002/17314.

Anthony, D.W., Brown, D.R., Khokhlov, A.A., Kuznetsov, P.F., Mochalov, O.D., 2016. A Bronze Age Landscape in the Russian Steppes: The Samara Valley Project. Cotsen Institute of Archaeology Press.

Anthony, D.W., 2007. The Horse, the Wheel, and Language: How Bronze-Age Riders from the Eurasian Steppes Shaped the Modern World. Princeton University Press. https://doi.org/10.2307/j.ctt7sjpn.

Artyuhova, O.A., Kurmankulov, Zh., Ermolaeva A.S., Erzanova, A.E., 2013. The complex of monuments in the Taldysai tract. Volume 1 [Комплекс Памятников в урочище Талдысай. Том I]. Almaty: Institute of Archaeology named after A.Kh. Margulan (in Russian).

Artemyev, D.A., Ankushev, M.N., 2019. Trace Elements of Cu-(Fe)-Sulfide Inclusions in Bronze Age Copper Slags from South Urals and Kazakhstan: Ore Sources and Alloying Additions. Minerals, 9, 746, 1-23. https://doi.org/10.3390/min9120746.

Avanesova, N.A., 2020. Archaeology of Central Asia. Neolithic and Bronze Age [Археология Средней Азии: Энеолит и Бронзовый Век]. Samarkand: SHABNAM OMAD NUR Publishing House (in Russian).

Avanesova, N.A., 2015.Ceramics of the settlement of miners-metallurgists of Zarafshan [Керамика поселениа горняков-металлургов Зарафшана]. History of material culture of Uzbekistan. Issue 39 [История материальной культуры Узбекистана. Выпуск 39]. Samarkand: Institute of Archeology of the Academy of Sciences of the Republic of Uzbekistan (in Russian), pp. 47-62.

Bachmann, H.G., 1982. The identification of slags from archaeological sites. London: University of London, Institute of Archaeology, Occasional publications, Volume 6.

Beisenov, A.Z., Yermolayeva, A.S., Duysenbay, D.B. 2017. Housing-workshop on the settlement of the Bronze times of Murzhyk (Central Kazakhstan) [Жилище-Мастерская На Поселении Эпохи Бронзы Мыржык (Центральный Казахстан)]. In Bazarov, B.V. and Kradin, N.N. (Eds.), Actual Problems of Archaeology And Ethnology Of Central Asia. Materials of the II International conference (Ulan-Ude, 4–6th December, 2017) [Актуальные Вопросы Археологии И Этнологии Центральной Азии Материалы II международной научной конференции (г. Улан-Удэ, 4–6 декабря 2017 г.)]. Ulan Ude: The Buryat Scientific Center SB RA, pp. 108-113 (in Russian).

Berdenov, S.A., 2008. Kazakhstan deposits of copper and tin and their development in the Bronze Age [Казахстанские месторождения меди и олова и их разработка в бронзовом веке]. Известия НАН РК. Сер. обществ. Наук. [Proceedings of the National Academy of Sciences of the Republic of Kazakhstan. Serie Societies. Science], pp. 42-55.

Boscher, L., 2016. Reconstructing the Arsenical Copper Production Process in Early Bronze Age Southwest Asia. PhD Thesis at UCL Institute of Archaeology.

Bourgarit, D., 2007. Chalcolithic copper smelting, in: La Niece, S., Hook, D., Craddock, P. (Eds.), Metals and Mines. Studies in Archaeometallurgy. London: Archetype Publications, pp. 3-14.

Box, S.E., Syusyura, B., Hayes, T.S., Taylor, C.D., Zientek, M.L., Hitzman, M.W., Seltmann, R., Chechetkin, V., Dolgopolova, A., Cossette, P.M., Wallis, J.C., 2012a. Sandstone copper assessment of the Chu-Sarysu Basin, Central Kazakhstan: U.S. Geological Survey Scientific Investigations Report 2010-5090-E, 1-63.

Box, S.E., Syusyura, B., Seltmann, R., Creaser, R.A., Dolgopolova, A., Zientek, M.L. 2012b. Dzhezkazgan and Associated Sandstone Copper Deposits of the Chu-Sarysu Basin, Central Kazakhstan. Econ. Geol., 16, pp. 303-328.

Calgaro, I., Radivojević, M. 2022. Chemical and microstructural analysis of experimental smelting debris produced in a Mid-Late Bronze Age shaft furnace replica from Taldysai, in: Yermolayeva, A.S, Rusanov, I.A. Experimental modelling of metallurgical furnaces in the site of Taldysai. Proceedings of the A.Kh. Margulan Institute of Archaeology, volume 4. Almaty: A.Kh. Margulan Institute of Archaeology (in English and Russian).

Chen, K., Liu, S., Li, Y., Mei, J., Shao, A., Yue, L., 2017. Evidence of arsenical copper smelting in Bronze Age China: a study of metallurgical slag from the Laoniupo site, central Shaanxi. J. Archaeol. Sci., 82, 31-32. https://doi.org/10.1016/j.jas.2017.04.006.

Chernykh, E.N., 2013. Nomadic cultures in the Mega-Structure of Eurasian World. Volume 1. [Культуры номадов в мегаструктуре Евразийского мира. Том 1], Moscow: Languages of the Slavs Cultures (in Russian).

Chernykh, E.N., 2011. Eurasian Steppe Belt: Radiocarbon Chronology and Metallurgical Provinces, in: Yalçın, Ü. (Ed.), Anatolian Metal V, Der Anschnitt, Beiheft 24. Bochum: Deutsches Bergbau-Museum, pp. 151-172.

Chernykh, E.N., 2008. The "Steppe Belt" of stockbreeding cultures in Eurasia during the Early Metal Age. Trabajos Prehist., 65, 2, 73-93. https://doi.org/10.3989/tp.2008.08004.

Chernykh, E.N., 2007. Kargaly V: Phenomenon and Paradoxes of Development [Каргалы: Феномен и парадоксы развития], Moscow: Language of Slavonic culture (in Russian).

Chernykh, E.N., 2004. Kargaly III: Gorny site. Archaeological materials, mining and metallurgy technology, archaeobiological studies [Каргалы. Том III. Селище Горный: археологические материалы, технология горно-металлургическогопроизводства, археобиологические исследования]. Moscow: Language of Slavonic culture (in Russian).

Chernykh, E.N., 2002a. Kargaly 1: Geological and geographical characteristics: History and discoveries, exploitation and investigations: Archaeological sites [Каргалы 1: Геолого-географические характеристики: История откритий, эксплуатации и иследований: Археологические памятник]. Moscow: Languages of Slavonic Cultures (in Russian).

Chernykh, E.N., 2002b. Kargaly 2: Gorny - the Late Bronze Age settlement. Topography, lithology, stratigraphy. Household, manufacturing and sacral structures. Relative and absolute chronology [Каргалы 2: Поселение эпохи поздней бронзы: Топография, литология, стратиграфия: Производственно-бытовые и сакралные сооружения: Относительная и абсолютная хронологиа]. Moscow: Languages of Slavonic Cultures (in Russian).

Chernykh, E.N., 1992. Ancient metallurgy in the USSR: the Early Metal Age. Translated by Sarah Wright. Cambridge: Cambridge University Press.

Chernykh, E.N., 1966. History of ancient metallurgy of Eastern Europe [История древнейшей металлургии восточной Европы]. Moscow: Science Publishing House (in Russian).

Chernykh, E.N., Kuzminykh, S.V., 1989. Ancient Metallurgy in the Northern Eurasia. Seyma-Turbino Phenomenon, Moscow [Древняя металлургия Северной Евразии (Сейминско-Турбинский феномем)]. Moscow: Nauka (in Russian).

Copper fields of Kazakhstan. Reference book [Месторождения меди Казахстана. Справочник], 1997. Edited by Abdulina, A.A., Bespaeva, Ch. A., Daukeeva, S.Zh. et al. Almaty: Committee of Geology and Subsoil Protection of the Ministry of Ecology and Natural Resources (in Russian).

Craddock, P. T., 1995. Early Metal Mining and Production, Edinburgh: Edinburgh University Press.

Craddock, P.T. and Meeks, N.D. (1987), Iron in ancient copper. Archaeometry, 29: 187-204. https://doi.org/10.1111/j.1475-4754.1987.tb00411.x.

Di Cosmo, N., 1996. Ancient Xinjiang Between Central Asia and China. The Nomadic Factor. Anthr. Archeol. Euras., 34, 4, 87-101. https://doi.org/10.2753/AAE1061-1959340487.

Donaldson, C.H., 1976. An experimental investigation of olivine morphology. Contributions to Mineralogy and Petrology, 57.

Erb-Satullo, N.L., Gilmour, B.J.J., Khakhutaishvili, N., 2014. Late Bronze and Early Iron Age copper smelting technologies in the South Caucasus: the view from ancient Colchis c. 1500-600 BC. J. Archaeol. Sci., 49, 147-159. https://doi.org/10.1016/j.jas.2014.03.034.

Erb-Satullo, N.L., Gilmour, B.J.J., Khakhutaishvili, N., 2015. Crucible technologies in the Late Bronze-Early Iron Age South Caucasus: copper processing, tin bronze production, and the possibility of local tin ores. J. Archaeol. Sci., 61, 260-276. https://doi.org/10.1016/j.jas.2015.05.010.

Frachetti, M., 2012. Multiregional Emergence of Mobile Pastoralism and Nonuniform Institutional Complexity across Eurasia. Curr. Anthropol., 53, 2-38. https://doi.org/10.1086/663692.

Frachetti, M. D., Evan Smith, C., Traub, C. M., Williams, T. 2017. Nomadic ecology shaped the highland geography of Asia's Silk Roads. Nature, 543, 193-198. https://doi.org/10.1038/nature21696.

Grigoriev, S., 2021. Andronovo problem. Studies of Cultural Genesis in the Eurasian Bronze Age. *Open Archaeology*, 7, pp. 3-36. doi:10.1515/opar-2020-0123.

Grigoriev, S.A., 2015. Metallurgical production in Northern Eurasia in the Bronze Age. Oxford: Archaeopress Publishing Ltd.

Grigoriev, S.A., 2000. Metallurgical production in the Southern Urals in the Middle Bronze Age. [Металлургическое производство на Южном Урале в эпоху средней бронзы], in: Ancient History of Southern Transurals. Book 1: Stone Age. The Bronze Age [Древняя история Южного Зауралья. Т. I: Каменный век. Эпоха бронзы]. Chelyabinsk: SUSU Publishing House, pp. 444-531 (in Russian).

Grigoriev, S.A., Rusanov, I.A., 1995. Experimental reconstruction of ancient metallurgical production, in: Arkaim. Research. Search. Discoveries [Экспериментальная реконструкция древнего металлургического производства, in: Аркаим. Исследования. Поиски. Открытия]. Chelyabinsk: Stone Belt Series, pp. 147-158 (in Russian).

Haak, W., Lazaridis, I., Patterson, N., Rohland, N., Mallick, S., Llamas, B., Brandt, G., Nordenfelt, S., Harney, E., Stewardson, K., et al., 2015. Massive migration from the steppe was a source for Indo-European languages in Europe. Nature, 522, 207-211. https://doi.org/10.1038/nature14317.

Hanks, B., Doonan, R., 2009. From Scale to Practice: A New Agenda for the Study of Early Metallurgy on the Eurasian Steppe. J. World Prehist., 22, 329. https://doi.org/10.1007/s10963-009-9031-5.

Hauptmann, A. 2020. Archaeometallurgy. Materials Science Aspects. Springer Cham. https://doi.org/10.1007/978-3-030-50367-3

Hauptmann, A., 2000. Reconstructing Ancient Smelting Processes: Applied Mineralogy in Archaeometallurgy, in: Rammlmair, D. (Ed.), Applied Mineralogy: in research, economy, technology, ecology and culture. Proceedings of the Sixth International Congress on Applied Mineralogy. Göttingen, pp. 29-31.

Hermes, T.R., Frachetti, M.D., Voyakin, D., Yermolaeva, A.S., Beisenov, A.Z., Doumani Dupuy, P.N., Papin, D.V., Matuzeviciute, G.M., Bayarsaikhan, J., Houle, J-L., Tishkin, A.A., Nebel, A., Krause-Kyora, B., Makarewicz, C.A., 2020. High mitochondrial diversity of domesticated goats persisted among Bronze and Iron Age pastoralists in the Inner Asian Mountain Corridor. PloSOne, 15, 5. https://doi.org/10.1371/journal.pone.0233333.

Kadyrbaev, M.K., 1983. Six years of work on Atasu [Шестилетние работы на Атасу], in: Merpert, N.Ya, Zdanovich, G.B. (Eds.), Bronze Age of the steppe of the Ural-Irtysh interfluve [Бронзовый век степной полосы Урало-Иртышского междуречья]. Chelyabinsk: ChelGU; BashGU, pp. 134-142 (in Russian).

Khazanov, A.M., 1994. Nomads and the Outside World. Second Edition. Madison: The University of Wisconsin Press.

Killick, D. 2014. Chapter 2. From Ores to Metals. In Roberts, B., Thornton, C. (Eds.), Archaeometallurgy in Global Perspective. Methods and Syntheses. NY: Springer New York, pp. 11-45.

Knapp, A.B., Kassianidou, V., 2008. The Archaeology of Late Bronze Age Copper Production - Politiko Phorades on Cyprus, in: Yalçın, Ü. (Ed.), Anatolian Metal IV. Bochum: Deutsches Bergbau-Museum Bochum, pp. 135-147.

Kohl, P.L., 2007. The making of Bronze Age Eurasia. Cambridge: Cambridge University Press.

Koryakova, L., Epimakhov, A., 2007. The Urals and Western Siberia in the Bronze and Iron Ages. Cambridge: Cambridge University Press.

Koucky, F. L., Steinberg, A. 1982. Ancient Mining and Mineral Dressing on Cyprus. In Wertime, T.A. and S.F. (Eds.), *Early Pyrotechnology: The Evolution of the First Fire-Using Industries*. Washington, D.C: Smithsonian Institution Press, pp. 149-180.

Kraus, S., Schröder, C., Klemm, S., Pernicka, E., 2015. Archaeometallurgical studies on the slags of the Middle Bronze Age copper smelting site S1, Styria, Austria, in: Hauptmann, A., Modarressi-Tehrani, D. (Eds.), Archaeometallurgy in Europe III. Proceedings of the 3rd International Conference. Bochum: Deutsches-Bergbau Museum, pp. 301-308.

Kurmankulov, Zh., Yermolayeva, A.S., Erzhanova, A.E. 2012. Taldysay - settlement of ancient metallurgists [Поселение Талдысай - Памятник древней металлургии]. Kazakhstan: Publishing house of the Academy of sciences of the Republic of Kazakhstan (in Russian).

Kuzmina, E.E., 2008. The Prehistory of the Silk Road. Philadelphia: University of Pennsylvania Press

Kuznetsova, E.F., Teplovodsakya, T.M., 1994. Ancient Metallurgy and pottery-making in Central Kazakhstan [Древняя Металлургия и Гончарсво Центрального Казахстана], Almaty: Gilim Publishing (in Russian).

Larreina-Garcia, D., Cech, B., Rehren, T., 2015. Copper Smelting in the Raxgebiet (Austria): A Late Bronze Age Alpine Industrial Landscape, in: Suchowska-Ducke, P., Scott Reiter, S., Vandkilde, H. (Eds.), Forging Identities. The Mobility of Culture in Bronze Age Europe, 1, pp. 213-219. London: Archaeopress.

Lechtman, H., Klein, S., 1999. The Production of Copper–Arsenic Alloys (Arsenic Bronze) by cosmelting: Modern Experiment, Ancient Practice. J. Archaeol. Sci., 26, 497-526.

Lechtman, H. 1991. The production of copper-arsenic alloys in the Central Andes: Highland ores and coastal smelters? Journal of Field Archaeology, 18, 43-76. https://doi.org/10.1179/009346991791548780.

Librado, P., Khan, N., Fages, A., Kusliy, M.A., Suchan, T., Tonasso-Calvière, L., Schiavinato, S., Alioglu, D., Fromentier, A., Perdereau, A. et al., 2021. The origins and spread of domestic horses from the Western Eurasian steppes. Nature, 598, 634-640. https://doi.org/10.1038/s41586-021-04018-9.

Liu, S., He, X., Chen, J., Zou, G., Guo, S., Gong, X., Rehren, T., 2020. Micro-slag and “invisible” copper processing activities at a Middle-Shang period (14th-13th century BC) bronze casting workshop. J. Archaeol. Sci., 122, 1-11. https://doi.org/10.1016/j.jas.2020.105222.

Margulan, A.Kh., 2020. Saryarka. Mining and metallurgy in the Bronze Age. Jezkazgan - Ancient and medieval metallurgical center [Сарыарка. Горное дело и металлургия в Эпоху Бронзы. Жезказган - Древний и Средневековый металлургический центр (городище Милыкудук)]. A. Kh. Margulan Institute of Archaeology: Almaty (in Kazakh, Russian and English).

Merkel, J., Shimada, I. 1988. Arsenical copper smelting at Batán Grande, Peru. IAMS, 12, 4-7.

Narasimhan, V. M., Patterson, N., Moorjani, P., Rohland, N., Bernardos, R., Mallick, S., Lazaridis, I., Nakatsuk, N., Olalde, I., Lipson, M. et al., 2019. The formation of human populations in South and Central Asia. *Science*, 365, 6457, 1-15. https://doi.org/10.1126/science.aat7487.

Park, J-S., 2020. Copper-based metallurgy as observed in metal objects excavated from the LBA site at Taldisai in Central Kazakhstan, in: Kurmankulov, Zh. (Ed.), Taldysai. Settlement of ancient metallurgists of the Late Bronze Age in the Ulytau Steppe. Collective Monograph [Талдысай - Поселение древних металлургов Позднегобронзого Века в Улитаиской степи]. Almaty: Institute of Archaeology named after A.Kh. Margulan, pp. 214-231 (in Russian).

Pearce, M., Merkel, S., Hauptmann, A., Nicolis, F., 2022. The smelting of copper in the third millennium cal BC Trentino, north-eastern Italy. Archaeological and Anthropological Sciences, 14, 10. https://doi.org/10.1007/s12520-021-01475-1.

Pernicka, E., Lutz, J., Stöllner, T., 2016. Bronze Age copper produced at Mitterberg, Austria, and its Distribution. Archaeologia Austriaca, 100, 19-55. 1 https://doi.org/0.1553/archaeologia100s19.

Radivojević, M., 2013. Archaeometallurgy of the Vinča culture: a case study of the site of Belovode in eastern Serbia. Hist. Metall., 47, 13-32.

Radivojević, M., Rehren, Th., Pernicka, E., Šljivar, D., Brauns, M., Borić, D., 2010. On the origins of extractive metallurgy: new evidence from Europe. J. Archaeol. Sci., 37, 2775-2787. https://doi.org/10.1016/j.jas.2010.06.012.

Radivojević, M., Roberts, B.,W., Pernicka, E., Stos-Gale, Z.A., Martinón-Torres, M., Vandkilde, H., Ling, J., Brandherm, D., Bray, P., Mei, J., Kristiansen, K., Rehren, Th., Shennan, S., Broodbank, C., 2019. The provenance, use and circulation of metals in the European Bronze Age: The state of debate. J. Archaeol. Res., 27, 131-185.

Rehren, Th., Boscher, L., Pernicka, E., 2012. Large scale smelting of speiss and arsenical copper at Early Bronze Age Arisman, Iran. J. Archaeol. Sci., 39, 1717-1727. https://doi.org/10.1016/j.jas.2012.01.009.

Rehren, Th., Radivojević, M., 2010. A preliminary report on the slag samples from Çamlıbel Tarlası. In: Schachner, A., Üstündağ, H., Dittman, R., Röttger, U., Wilhelm, G., Schoop, U.-D., Marsh, B., Rehren, Th., Radivojević, M. (Eds.), 2010. Die Ausgrabungen in Boğazköy-Hattuša 2009, vol. 6. Archäologischer Anzeiger, pp. 207-216.

Rostoker, W., Pigott, V.C., Dvorak, J., 1989. Direct reduction to copper metal by oxide/sulfide mineral interaction. Archeomaterials, 3, 69-87.

Rovira, S. 1999. Una propuesta metodológica para el studio de la metalugia prehistórica: el caso de Gorny en la región de Kargaly (Orenburg, Rusia). Trabajos Prehist, 56, 2, 85-113. https://doi.org/10.3989/tp.1999.v56.i2.277.

Saptaev, K.I., 1956. The main specific features of the geology and metallogeny of the Dzhezkazgan-Ulytau region (sheets M-42-B and L-42-A). Materials for metallogenic prognostic map of Central Kazakhstan. [Основные специфические особенности геологии и металлогении Джезказган-Улутауского района (листы М-42-В и L-42-А). Материалы к металлогенической прогнозной карте Центрального Казахстана]. Almaty (in Russian).

Satpaeva, M.K. 2007. Mercury-arsenic-silver mineralization in the lower horizons of Dhzezkazgan [Ртутно-мышьяково-серебряная минерализация на нижних горизонтах Жезказгана]. Izvestiya NAS RK. Geological series [Известия НАН РК. Серия геологическая], 5, pp. 17-36 (in Russian).

Shishlina, N.I., Orfinskaya, O.V., Hommel, P., Zazovskaya, O.P., Ankusheva, P.S., van der Plicht, J. 2020. Bronze Age Wool Textile of the Northern Eurasia: New Radiocarbon Data. *Nanotechnologies in Russia*, 15 (9-10), 629-638. https://doi.org/10.1134/s1995078020050146.

Silvestri, E., Bellintani, P., Nicolis, F., Bassetti, M., Biagioni, S.,Cappellozza, N., Degasperi, N., Marchesini, M., Martinelli, N. et al., 2015. New excavation at the sites in Trentino, Italy: archaeological and archaeobotanical data, in: Hauptmann, A., Modarressi-Tehrani, D. (Eds.), Archaeometallurgy in Europe III, Proceedings of the 3rd International Conference. Bochum: Deutsches-Bergbau Museum, pp. 369-376.

Slag Atlas, 1995. 2nd Edition, Verein Deutscher Eisenhüttenleute (Eds.). Düsseldorf: Verlag Stahleisen GmbH.

Stöllner, T. 2018. What is an Ore Deposit? Approaches from Geoscience and Archaeology in Understanding the Usage of Deposits. Metalla, 24.2, pp. 87-100. https://doi.org/10.46586/metalla.v24.2018.i2.87-110.

Stöllner, T., Bode, M., Gontscharov, A., Gorelik, A., Hauptmann, A., Prange, M. 2013a. Metall und Metallgewinnung der Bronze- und Früheisenzeit in Zentral- und Ostakasachstan, in: Stöllner, T., Samashev, Z. (Eds.), Unbekanntes Kasachstan. Archäologie im Herzen Asiens. Bochum: Deutsches Bergbau-Museum Bochum, pp. 383-398.

Stöllner, T., Samashev, Z., Berdenov, S., Cierny, J., Doll, M., Garner, J., Gontscharov, A., Gorelik, A., Hauptmann, A., Herd, R., Kusch, G. A., Merz, V., Riese, T., Sikorski, B., Zickgraf, B. 2013b. Tin from Kazakhstan - Steppe Tin for the West?, in: Yalçın, U., Wirth, C. (Eds.), Anatolian Metal V. Bochum: Deutsches Bergbau-Museum Bochum, pp. 231-252.

Thornton, C.P., Rehren, T., Pigott, V.C., 2009. The production of speiss (iron arsenide) during the Early Bronze Age in Iran. J. Archaeol. Sci., 36, 308-316. https://doi.org/10.1016/j.jas.2008.09.017.

Tkachev, V.V, 2019. Mining and Metallurgical Production in the Structure of Economic and Cultural Models of the Western Periphery of Alakul Culture. Urals Historical Bulletin [Уралский Исторический Вестник], 62, 1, 38-47. https://doi.org/10.30759/1728-9718-2019-1(62)-38-47 (in Russian).

Tkachev, V.V., Yuminov, A.M., Baitleu, D.A., 2014. Development of Copper Ore Resources of Western Kazakhstan in the Bronze Age. In: Baitleu, D.A., (Ed.), Cultural and historical processes in the Kazakh steppes in antiquity and the Middle Ages: traditions and innovations [Қазақ даласындағы көне және ортағасырлық тарихи-мәдени үдерістер: дәстүрлер мен инновациялар. – Культурно-исторические процессы в Казахских степях в древности и средневековье: традиции и инновации.]. Astana: Branch of the Institute of Archaeology named after A.Kh. Margulan, pp. 97-115 (in Kazakh and Russian).

Vandkilde, H., 2017. Small, medium and large. Globalization perspectives on the Afro-Eurasian Bronze Age, in: Hodos, T. (Ed.), The Routledge Handbook of Archaeology and Globalization. Routledge, pp. 509-521.

Vandkilde, H., 2016. Bronzization: The Bronze Age as Pre-Modern Globalization, in: Bertèmes, F., Della Casa, P., Schier, W., Wemhoff, M. (Eds.), Praehistorische Zeitschrift, 91. De Gruyter, pp. 103-123.

Yermolayeva, A.S., 2020. Introduction. History of research [Введение. История исследований], in: Kurmankulov, Zh. (Ed.), Taldysai. Settlement of ancient metallurgists of the Late Bronze Age in the Ulytau steppe. Collective monograph [Талдысай. Поселение древних металлургов Позднебронзого Века в Улытауской степи. Коллективная монография]. Almaty: Institute of Archaeology named after A.Kh. Margulan, pp. 3-17.

Yermolayeva, A.S., 2017. To the problems of metal production from the Bronze age of Kazakhstan [К проблемам металлопроизводства эпохи бронзы Казахстана]. World of Great Altai [Мир Большого Алтая], 3, 4, 480-493 (in Russian).

Yermolayeva, A.S., 2016. Petrovka-Nurtay cultural horizons in the settlment Taldysai [Петровско-Нуртайске жилища-мастерские на поселении Талысай], in: Kurmankulov, Zh., Beisenov, A.Z. (Eds.), *Actual problems of Eurasian archaeology* [*Актуальные проблемы археологии Евразии*]. Almaty: Institute of Archaeology named after A. Kh. Margulan, pp. 126-142 (in Russian).

Yermolayeva, A.S., Erzhanova, A.E., Dubyagina, E.V., 2020a. Chapter 1. Industrial and housing complexes. Characteristics of the heat-engineering structures [Глава 1. Производственно-жилищные комплексы. Характеристика теплотехнических сооружений], in: Kurmankulov, Zh. (ed.), Taldysai. Settlement of ancient metallurgists of the Late Bronze Age in the Ulytau steppe. Collective monograph. [Талдысай. Поселение древних металлургов Позднебронзого Века в Улытауской степи. Коллективная монография]. Almaty: Institute of Archaeology named after A.Kh. Margulan, 18-71 (in Russian).

Yermolayeva, A.S., Erzhanova, A.E., Kurmankulov, Zh., Rusanov, I., 2013. Die Siedlung Taldysaj ein Denkm al der technischen Kultur der alten Stämm e der Region Žezk azgan-Ulytau (Zentralkasachstan), in: Stöllner, T., Samashev, Z. (Eds.), Unbekanntes Kasakhstan. Bochum: Deutsches Bergbau-Museum Bochum, pp. 441-454.

Yermolayeva, A.S., Kaliyeva, Z.S., Dubyagina, E.V., 2018. Cultural attribution of the dwelling-workshop on the basis of the Taldysay settlement ceramics analysis [Культурная атрибуция жилища-мастерской на поселении Талдысай на основе анализа керамики]. Samara Journal of Science [Самарский научный вестник], 7, 3, 24, 269-275 (in Russian).

Yermolayeva, A.S., Kuzmynikh, S.V., Dubyagina, E.V., 2020b. Tracing the Origins of Metallurgy to the Mining Regions of Kazakhstan [Миграционное происхождение технологий металлопроизводства Казахстанской горно-металлургической области]. Stratum Plus, pp. 103-116 (in Russian).

Yermolayeva, A.S., Kuzminykh, S.V., Park, J-S., Dubyagina, E.V., 2019. Late Bronze Age Weapons from Foundry Workshops of Taldysay Settlement, Central Kazakhstan [Предметы вооружения позднего бронзового века из мастерских литейщиков поселения Талдысай в Центральном Казахстане]. Stratum Plus, 109-120 (in Russian).

Yermolayeva, A.S., Rusanov, I.A., 2022. Experimental modelling of metallurgical furnaces of the settlement Taldysai. Proceedings of the Institute of Archeology named after A.Kh. Margulan. Book 4 [Эксперименальное моделирование металлургиеских печей поселения Талдысай. Труды Института археологии им А.Х. Маргулана. Т. IV.]. Almaty: Institute of Archaeology named after A.Kh. Margulan (in Russian).

Zaykov, V.Z., Yuminov, A.M., Ankushev, M.N., Epimakhov, A.V., 2013. Slags, ores and bronzes from the Kamennyi Ambar archaeological microdistrict: sources of ores for ancient metallurgy in the southern Urals, in: Krause, R., Koryakova, L.N. (Eds.), Multidisciplinary investigations of the Bronze Age settlements in the Southern Trans-Urals (Russia). Bonn: Verlag Dr. Rudolf Habelt GmbH, pp. 187-201.